This is to certify that the
thesis entitled

INVESTIGATION INTO THE ABILITY OF THE BLUESKY SMOKE MODELING FRAMEWORK IN SIMULATING SMOKE IMPACTS FROM WILDFIRES

presented by

Lesley Adele Fusina

has been accepted towards fulfillment
of the requirements for the

M.S. degree in Geography

Major Professor's Signature

May 22, 2008

Date

INVESTIGATION INTO THE ABILITY OF THE BLUESKY SMOKE MODELING FRAMEWORK IN SIMULTAING SMOKE IMPACTS FROM WILDFIRES

By

Lesley Adele Fusina

A THESIS

Submitted to
Michigan State University
in partial fulfillment of the requirements
for the degree of

MASTER OF SCIENCE

Department of Geography

2008

ABSTRACT

INVESTIGATION INTO THE ABILITY OF THE BLUESKY SMOKE MODELING FRAMEWORK IN SIMULTAING SMOKE IMPACTS FROM WILDFIRES

By

Lesley Adele Fusina

Wildland fires are necessary for regeneration and stimulation of soils and plant growth as well as for forest management practices. In the United States, increased fire suppression and prescribed burn activities have decreased the number of total fires over time but, instead of seeing a reduction in fire size as well, fires are becoming larger. These large fires have the potential to release substantial amounts of smoke which can lead to poor air quality and reduce visibility. The BlueSky Smoke Modeling Framework is designed to assist fire and air quality managers in predicting the timing, location and magnitude of smoke impacts from wildland fires. In this study, large wildfire episodes in California were used to examine BlueSky's ability to accurately predict timing and location of wildfire smoke impacts. This analysis is necessary as BlueSky is being used more and more as a one-stop shopping tool for predicting smoke concentration and emissions across the United States, but the accuracy and uncertainties in BlueSky predictions are still largely unknown. This study found BlueSky able to highlight areas of potential smoke impact by reliably predicting long-range transport of wildfire smoke plumes. The magnitudes of potential smoke impacts were less reliable with accurate predicted surface $PM_{2.5}$ concentrations occurring infrequently and only when observed magnitudes were greater than 10 $\mu g\ m^{-3}$.

ACKNOWLEDGEMENTS

The completion of this thesis would not be possible without the guidance, support and help from some very important people. First and foremost, to my advisor, Dr. Shiyuan Zhong, thank you for the opportunity to pursue this research and the constant editing and support along the way. To Xindi Bian, without whom, I would still be crying in my office trying to get the model to run! Your help will forever be appreciated. I would also like to thank Wenqing Yao, your expertise in MATLAB, willingness to help, and analysis suggestions helped to make this project a success. Importantly, much thanks is given to the USDA Forest Service Pacific Northwest AirFire Team, especially Robert Soloman, Tara Strand and Sim Larkin, without your expertise and vision, none of what I achieved would have been possible. Additionally, I'd like to thank Dr. Jay Charney for his revisions, knowledge and challenging questions, you certainly kept me on my toes. To the rest of my committee members, Dr. Julie Winkler and Dr. Jeff Andresen, you've been with me six years now and have always looked out for my best interest. Without your help I would not be where I am today. Finally and most importantly, to my family and friends. Your support and words of encouragement are the reason this thesis is completed. I will never be able to repay you for your constant energy, patience and ability to say just the right thing at just the right time.

TABLE OF CONTENTS

List of Tables vi

List of Figures viii

PART I. INTRODUCTION 1
Thesis Objective 3

PART II. BACKGROUND 6
Literature Review 6
Smoke Dispersion Modeling 6
The BlueSky Smoke Modeling Framework 17
Model Description 23
$PM_{2.5}$ Concentrations and Smoke Trajectory Simulations 23
Summary 27

PART III. NORTHERN CALIFORNIA, AUGUST 2006 28
Introduction 28
Methods 30
Study Area 30
Observational Data 32
Satellite Observations 33
Model Simulations 36
Results and Discussion 37
Wildland Fires and Synoptic Weather Conditions during the Study Period 37
Meteorological Fields 40
Smoke Plume and $PM_{2.5}$ Prediction 49
Summary and Conclusions 55

PART IV. SOUTHERN CALIFORNIA, OCTOBER 2007 58
Introduction 58
Methods 61
Study Area 61
Model Setup and Simulations 63
Surface and Satellite Observations 65
Results and Discussion 75
Wildland Fires and Synoptic Weather Conditions during the Study Period 75
Meteorological Fields 77
Smoke Plume and $PM_{2.5}$ Predictions 86
Summary and Conclusions 97

PART V. CONCLUSIONS 100
Summary 100
Study Limitations 103
Future Work 105

REFERNCES 108

LIST OF TABLES

2.1 Temporal allocation of acres burned in a day for wildfires. Data developed by the Western Regional Air Partnership (from WGA/WRAP, 2005) 26

3.1 Geographic station information for meteorological and $PM_{2.5}$ observations 35

3.2 BlueSky Input Information 37

3.3 Meteorological comparison statistics for surface temperature, mixing ratio and wind speed 46

4.1 Meteorological observation station geographic information 68

4.2 $PM_{2.5}$ observation station geographic information 72

4.3 Meteorological comparison statistics for surface temperature, mixing ratio and wind speed 82

LIST OF FIGURES

2.1 Fire modeling includes fire environment, fire characteristics, first-order fire effects and second-order fire effects. Examples are given for each category (modified from Andrews *et al*, 2001; pg. 345) 8

2.2 Elements of smoke dispersion models (from Breyfogle and Ferguson, 1996; pg 2) 9

2.3 Image analysis (left) of smoke plume on night of March 20, 1997 and PB-Piedmont simulated smoke (right) at (a) 2150 LST, (b) 2215 LST, (c) 2255 LST and (d) 2354 LST (modified from Achtemeier, 2006; pg. 92) 12

2.4 Schematic of modeling framework. Dotted arrows indicate interactions which are turned off or for which default values are assumed (from McKenzie *et al*, 2006; pg 281) 14

2.5 Observed and predicted $PM_{2.5}$ concentrations (left) a monitoring site in Idaho and the corresponding predicted plume concentration contours (right) during August 25, 2006 (from Jain *et al*, 2007; pg. 6756) 16

2.6 Maximum average and ground concentrations for the Rex Creek wildfire for the period of August 19-26, 2006 when the fire is (a) treated as a single fire, (b) split into 5 fires and (c) split into 10 fires. In all cases the total area burned is the same (from Larkin *et al*, 2007) 21

2.7 Components of the BlueSky modeling system 24

3.1 Terrain map of northern California and southern Oregon, including locations of observational meteorological and $PM_{2.5}$ stations. The black box indicates the simulated 4km domain 31

3.2 Plots of 500 hPa height (left) and wind speed (right) synoptic plots at 12Z (0400 PST). Light shading in the wind speed panels (right) indicates weaker 500 hPa wind speeds while darker shading indicates stronger wind speeds. Contours in the left panel represent 500 hPa isoheights 39

3.3 Simulated and observed hourly temperature (top), dewpoint temperature (center), and wind speed (bottom) at all fifteen surface meteorological stations used within this study. Gray dots are the day time values while the black dots are night time values 41

[1] Note that some images in this thesis are presented in color

3.4 Time series plots of surface temperature, wind speed and wind direction at three locations which show (a) the typical MM5 simulated pattern, (b) the pattern observed at stations located along the west coast, and (c) the pattern seen in the northern stations located in diverse terrain. Black dotted lines and upside down triangles (in wind direction time series) represent the observations while gray lines and x's (in wind direction) represent MM5 simulated surface meteorological conditions 43

3.5 Upper level patterns at 00Z (1600 PST) Medford, Oregon station at three different dates (a) August 21, 2006, (b) August 29, 2006, and (c) August 31, 2006. Variables examined are theta, mixing ratio, wind speed and wind direction; all plotted against height. Black dotted lines and upside down triangles (wind direction) represent observations while gray lines and x's (wind direction) represent MM5 simulated meteorological conditions 48

3.6 The images across the top show BlueSky visual output of surface $PM_{2.5}$ concentrations for three days (a) August 21, (b) August 29 and (c) August 31. The middle images show the corresponding satellite data taken from MODIS hazard mapping system (HMS), where gray shading indicates significant smoke plumes. Darker shades of gray represent higher concentrations of smoke. The bottom images are the aerosol optical depth data for each day, also taken from MODIS. Warmer colors indicate a higher concentration of aerosol within the atmosphere 50

3.7 Hourly $PM_{2.5}$ concentrations at the 8 monitoring stations located in northern California and southern Oregon. Solid black lines represent the observed adjusted concentrations of $PM_{2.5}$ while the gray dotted lines indicate the BlueSky estimated $PM_{2.5}$ concentrations..... 53

4.1 Modeling domains used within this study. D01 is the 36km domain, D02 is the 12km domain and D03 is the 4km domain. The 12km and 4km domains are one-way nested domains..... 64

4.2 Hourly data from 75 surface meteorological stations and twice daily soundings from the 6 upper air stations were used to validate MM5 predictions during October 15 – 30, 2007. The black box indicates the 4km one-way nested domain used for the simulations. Black circles indicate surface stations while red triangles indicate an upper air station 67

4.3 Surface particulate matter ($PM_{2.5}$) monitoring stations where hourly $PM_{2.5}$ data was obtained from the AIRNow monitoring sensors (circles) and the California Air Resources Board (ARB) monitoring sensors (stars). The black box indicates the 4km one-way nested domain used for the simulations 71

4.4 Plots of 500 hPa height (left) and wind speed (right) synoptic plots at 00Z (1600 PST). Light shading in the wind speed panels (right) indicates weaker 500 hPa wind speeds while darker shading indicates stronger wind speeds. Contours in the left panel represent 500 hPa isoheights 76

4.5 (a) Simulated and observed hourly temperature (top), mixing ratios (center), and wind speed (bottom) at all surface meteorological stations. Each circle indicates an hourly daytime average (0700 PST to 1900 PST) 78

4.5 (b) Simulated and observed hourly temperature (top), mixing ratios (center), and wind speed (bottom) at all surface meteorological stations. Each circle indicates an hourly nighttime average (2000 PST to 0600 PST) 79

4.4 Comparison of upper level profiles at 1600 PST (00Z) at the San Diego, CA rawinsonde site. Black circles represent observations. Light gray solid lines and circles (wind direction) represent MM5 simulated meteorological conditions initialized with Eta output. Darker gray dashed lines and circles (wind direction) represent MM5 simulations initialized with NARR output 85

4.7 (a) Satellite images taken from the MODIS Hazard Mapping System (HMS) for October 24 – 27, 2007. Gray shading indicates significant smoke plumes. Darker shades of gray represent higher concentrations of smoke. Corresponding BlueSky images are total $PM_{2.5}$ concentrations for the same days for the hours of 1300 PST to 2300 PST for (b) Eta MM5 initialization data and (c) NARR MM5 initialization data. Warmer colors indicate higher concentrations of $PM_{2.5}$ 87

4.8 (a) MODIS/GASP Aerosol Optical Depth (AOD) images at 1500 PST (2300Z) for October 24 - 27, 2007 with corresponding BlueSky simulated smoke plumes for (b) Eta MM5 initialization data and (c) NARR MM5 initialization data. Warmer colors in the AOD images indicate areas of higher aerosol concentrations. Warmer colors within the BlueSky images indicate higher levels of surface $PM_{2.5}$ concentration 89

4.9 (Left) Eta simulated and observed local time rate change of $PM_{2.5}$ concentrations at four monitoring sites within the domain. Black lines represent observed $PM_{2.5}$ and colored lines represent BlueSky simulated $PM_{2.5}$ concentrations. (Right) Corresponding surface meteorological stations. Black triangles represent observations while gray lines and stars represent MM5 simulated temperature (Temp), wind speed (Wspd), and wind direction (Wdir) 92

4.10 (Left) Eta simulated and observed local time rate change of $PM_{2.5}$ concentrations at four monitoring sites within the domain. Black lines represent observed $PM_{2.5}$ and colored lines represent BlueSky simulated $PM_{2.5}$ concentrations. (Right) Corresponding surface meteorological stations. Black triangles represent observations while gray lines and stars represent MM5 simulated temperature (Temp), wind speed (Wspd), and wind direction (Wdir) 94

PART I

INTRODUCTION

Fire is an important ecological process that dramatically affects both forested and non-forested ecosystems around the world. Naturally occurring fires are an integral component of the carbon cycle. They promote regeneration of threatened/endangered habitats, stimulate growth of many plant species, and also aid state and local agencies in management efforts of forest undergrowth (i.e. wildfires reduce dead and downed material to make room for new growth). Recently, humans have influenced these natural fire regimes through management strategies, such as prescribed burning. These strategies decrease the number of large catastrophic wildfires, but increase the overall size of wildfires (Minnich 1987; Odion et al. 2004). Wildfires also present a major threat to human populations who live near forested regions where the loss of home, property and life can be a direct result of uncontained wildfires. Secondary threats, such as decreased visibility and poor air quality also arise due to smoke emissions from the burning of biomass. The nature of wildland fires and their impacts on ecosystems and the people living in or near ecosystems complicates many aspects of fire management decisions.

Tools available for fire managers to help balance often conflicting management goals are prescribed burns and Wildland Fire Use (WFU) fires. Prescribed fires are those set for a specific management purpose, most often to remove down and dead undergrowth to reduce the risk of catastrophic wildfires or to develop or maintain habitat for threatened and endangered species. WFU fires are wildfires that ignite naturally and are allowed to burn under strict monitoring without suppression in locations where a fire is an important component of the ecosystem. If a WFU fire becomes a threat to a

community or begins to grow out of control, fire suppression activities begin. While the prescribed and WFU fires are tools that fire managers can use to mitigate the direct threats of wildfires, secondary threats due to smoke release must also be addressed.

Most of the wildfires in the United States occur in western states, which also include some of the worst air quality regions in the country (Association 2007). 16 of the 25 most polluted counties and over half of the U.S. cities cited on the worst ozone and particulate matter (PM) concentration lists are located in California. Considering southern California's synoptic circulation patterns, large population, and air quality degradation as a result of smoke contributions, California is often at risk of exceeding the national air quality standards set by the EPA.

Smoke constituents include gases, such as carbon monoxide, carbon dioxide, methane, and particulate matter (PM). The PM component of smoke is responsible for most of the smoke-induced undesirable physiological effects that occur within our body (Rapp 2006). $PM_{2.5}$ is particulate matter that is less than or equal to 2.5 microns in diameter. Due to its small size, $PM_{2.5}$ passes readily into the human respiratory system. Those most affected by increased levels of $PM_{2.5}$ are children, the elderly and those with weakened immune systems. Health effects associated with increased levels of $PM_{2.5}$ include eye and throat irritation, coughing, reduced lung function, blocked and runny noses, and in extreme cases, mortality (EPA 2003). In addition to the health impacts, PM can also greatly decrease visibility both locally and regionally (Malm, Day, and Kreidenweis 2000). Smoke impacts vary depending on fire location, types of fuel, and current and past weather conditions.

The BlueSky Smoke Modeling Framework is a tool that is used to aid smoke management of wildland fires (prescribed fires and wildfires) (Ferguson, Peterson, and Acheson 2001). Developed by the USDA Forest Service AirFire Team under the National Fire Plan, BlueSky links together five component models (fuel load, fire behavior, emissions, smoke dispersion and meteorology) to simulate the cumulative impacts of smoke in the form of PM concentration. BlueSky output is employed by operational fire managers and air quality regulators to help make 'go' and 'no-go' decisions related to prescribed burns, to assess the status of a WFU fire, and to support wildfire suppression strategies. While BlueSky is widely used by fire managers and air quality regulators, quantitative studies of BlueSky predictions are limited. The goal of this study is to investigate BlueSky's predictive capacity by simulating the smoke impacts from two extreme wildfire events that occurred in California in August, 2006 and October, 2007 and compare the BlueSky PM predictions with in-situ and remotely sensed observational data.

Thesis Objective

This thesis is composed of two case studies. The first case study is concerned with an outbreak of fires that occurred in northern California during late summer of 2006. The first goal of this case study is to evaluate the ability of the BlueSky Smoke Modeling Framework to accurately simulate smoke plume trajectories and $PM_{2.5}$ concentrations during this outbreak. Secondly, since northern California is characterized by varying and rough topography, the evaluation results will contribute to our knowledge of BlueSky ability to deal with varying terrain when simulating smoke movement, as BlueSky's

performance under those conditions is not well known. The second case study simulates wildfires that occurred in southern California in October of 2007. This case study is a first step at evaluating individual model components to assess how changes in these components affect the smoke plume trajectories and surface concentrations. The meteorological model used in BlueSky is evaluated using two different initialization data sets to see how different meteorological conditions affect the simulated smoke plumes. This evaluation will help assess the sensitivity of the BlueSky predictions to inputted meteorological data. The first dataset is the National Center for Environmental Prediction (NCEP) 40 km Eta data series and the second is the NCEP's North American Regional Reanalysis (NARR) 32 km data set. The BlueSky Smoke Modeling Framework is only as good as its individual components and the subsequent input information each provides. For example, the meteorological model provides predictions of surface and upper level wind speeds and directions, which are then inputted into the dispersion and trajectory models. If the wind speeds and/or directions are not accurate then one cannot expect the BlueSky predicted smoke plume trajectories and locations to be accurate. Analysis of each component's reliability and accuracy is necessary so that improvements can be made to each component, and subsequently to BlueSky predictions as well. In this study the following research questions will be addressed:

- Is the BlueSky Smoke Modeling Framework able to accurately predict wildfire smoke trajectories and timing of smoke impacts?

- Does BlueSky accurately predict surface $PM_{2.5}$ concentrations?

- Are BlueSky smoke plume and concentration predictions sensitive to the input data used within the meteorological model?

As stated above, this project helps to fill an information void that exists in the accuracy and sensitivity of the BlueSky Smoke Modeling Framework. In depth studies of model performance are missing from the literature. BlueSky has not been validated for different regions of the United States, since most existing literature focuses mainly on the Pacific Northwest region where BlueSky was initially developed. This project will provide results of BlueSky's predictive capabilities in regions of varying topography (northern California) and dense population (southern California).

Background information including a literature review of smoke dispersion modeling and the BlueSky framework and model descriptions are provided in Part II. Parts III and IV describe the case studies outlined previously. Part V summarizes the overall research conclusions and implications, study limitations and suggestions for future work within this research area.

PART II

BACKGROUND

Literature Review

The following section reviews the published literature on smoke dispersion modeling. The first part focuses on research and issues associated with smoke dispersion modeling. Next, literature and evaluation efforts of the BlueSky Smoke Modeling Framework will be presented in the second part.

Smoke Dispersion Modeling

Fire effects, defined by Reinhardt *et al* (2001), are the results of the combustion process. Fuel consumption, plant mortality, soil heating, erosion, nutrient cycling, vegetation succession and smoke production and dispersion are some important fire effects. Smoke dispersion is considered a second-order fire effect, one that occurs over longer time frames (days to months) and is located greater distances from the fire (Reinhardt, Keane, and Brown 2001; Andrews and Queen 2001). Secondary fire effects are modeled from, and dependent upon, inputs from the fire environment, fire characteristics and first order fire effects models (those effects measured within a few days and appear in a close proximity to the fire) (Figure 2.1). Because of this dependent nature, secondary fire effect's are difficult to model (Reinhardt, Keane, and Brown 2001).

Fire effects and behavior models are useful when assessing the risks from wildfire smoke to short and long-term air quality, ecosystem health and risks to surrounding communities. Although the terms are sometimes used interchangeably, fire behavior models and fire effects models are different with respect to their data inputs. Fire

behavior models provide a description of qualities of fuels that contributes to fire spread near the flaming front of the fire (Reinhardt, Keane, and Brown 2001). These fuels dictate the direction, rate and area of fire spread. While fire effects models also use knowledge of how the fire is spreading, the quantitative nature of these models also considers what remains burning after a fire front has passed (Reinhardt, Keane, and Brown 2001). In both types of modeling, an evaluation of the way fuel burns (Andrews and Queen 2001) and the associated impacts of each burn pattern is analyzed.

To predict smoke emissions and dispersion, estimates of smoke production (considered a first-order effect), terrain data and meteorology are necessary (Reinhardt, Keane, and Brown 2001). Of these, McGrattan (2003) indicates that terrain height and the mixing layer depth are most important for predicting wildfire smoke impacts. While this may be true, it is also essential that dispersion models integrate fire progression, fire emissions, atmospheric flow, smoke dispersion and chemical reactions (Miranda 2004). Figure 2.2 illustrates the basic components of a smoke model. Smoke dispersion models created specifically for wildland biomass burning include: SASEM (Sestak and Riebau 1988), VSMOKE (Lavdas 1996), CALPUFF (Scire, Strimaitis, and Yamartino 2000), and TSARS plus (Hummel and Rafsnider 1995). These models vary in complexity and have differing advantages and disadvantages. Breyfogle and Ferguson (1996) conducted a detailed evaluation of these smoke dispersion models. The following is a brief overview of their findings, highlighting the limitations in smoke dispersion modeling.

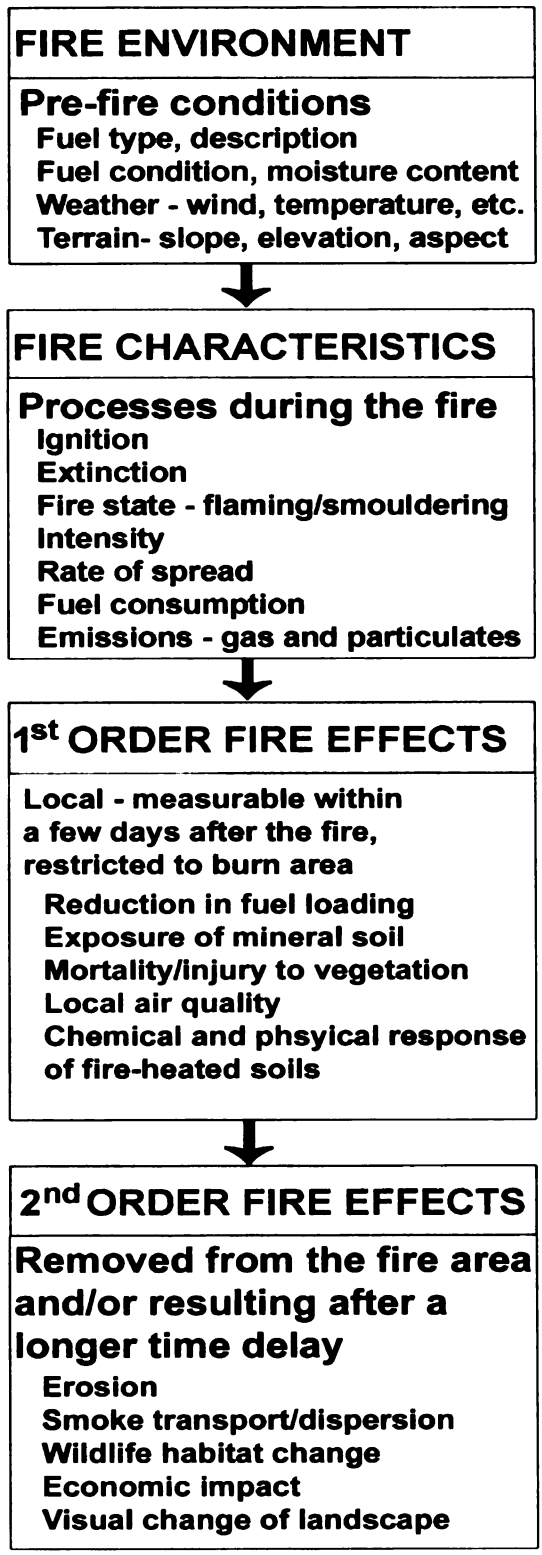

Figure 2.1 Fire modeling includes fire environment, fire characteristics, first-order fire effects and second-order fire effects. Examples are given for each category (modified from Andrews *et al*, 2001; pg. 345).

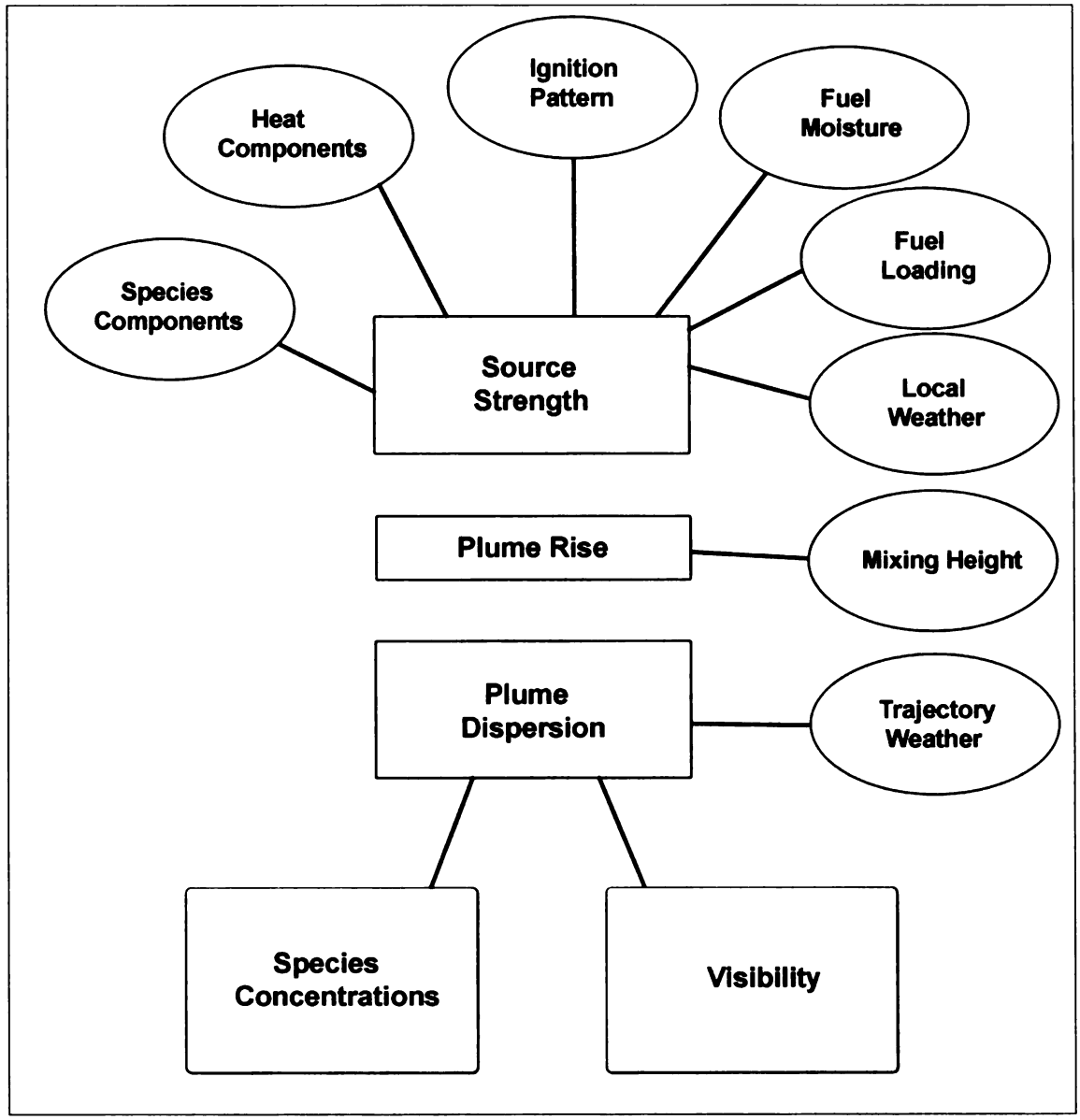

Figure 2.2 Elements of smoke dispersion models (modified from Breyfogle and Ferguson, 1996; pg 2).

CALPUFF, a multilayer, multispecies, non-steady state Gaussian puff dispersion model, and TSARS plus, a complex terrain wind-field model driving gaussian puffs for pollutant dispersion, account for complex terrain by interpolating observations to a 3-D grid (Breyfogle and Ferguson 1996). CALPUFF performed well in Breyfogle and

Ferguson's (1996) evaluation for a variety of factors: it has many different alternatives for model input and it can simulate an unlimited number of burns over an unlimited area (ideal for large-scale planning activities). CALPUFF, however, has only two options for calculating dispersion, both of which are based on Gaussian approximations, which may make it difficult to research all types of biomass burning. TSARS plus has similar model components as CALPUFF, but unlike CALPUFF, TSARS plus includes five different dispersion calculations that enable modeling of different types of biomass burning. Unfortunately, TSARS plus is domain dependent, meaning it can be applied to Wyoming only. Also, the usefulness of TSARS plus in large-planning efforts is hampered by the limit to the number of fires allowed to burn at one time. The major disadvantage and limitation of both of these models is that the difficult configuration and tedious input requirements often deter those with limited computer proficiency.

VSMOKE, a dispersion model only that was originally created to estimate potential visibility reduction for motorists, and SASEM, a screening tool for prescribed burns, utilize a simpler approach than CALPUFF and TSARS plus, by facilitating their use to anyone with limited to no computer experience (Breyfogle and Ferguson 1996). Both models can simulate one burn at a time, which is useful in screening individual burns. The simplistic nature of VSMOKE and SASEM, however, is also a limitation, as both models are restricted to areas where the terrain is relatively flat and they rely upon weather-observation data input directly by the user, compared to meteorology inputs estimated from a numerical model. These models are continually being modified so that improvement is made in both the inputs requirements from the user, as well as, in the

outputs of smoke plume and concentration predictions themselves (Breyfogle and Ferguson 1996).

In efforts to improve smoke dispersion models, many different frameworks have been tested. One such effort was to create a model that is more regional or location specific. Achtemeier (2005) describes a fine scale, smoke tracking model called Planned Burn-Piedmont (PB-Piedmont) valid for regions within the Piedmont plateau in the south-east US from Maryland to Alabama. The Piedmont is a low plateau roughly 100-300 km wide and 1500 km that separates the Atlantic Coastal Plain and Gulf Coastal Plain from the Appalachian Mountains. PB-Piedmont outputs high resolution space and time predictions of smoke movement within shallow layers at the ground. While PB-Piedmont is designed to work only when weather conditions are conducive to smoke entrapment (ie. at night with clear skies and light winds) and over certain geographical regions, it is capable of accurately capturing and simulating the movement of smoke plumes (Figure 2.3). This model however, is only concerned with simulating the movement of smoke plumes and not the smoke concentrations (Achtemeier 2005). PB-Piedmont exemplifies the usefulness and limitations of creating a model that is location specific. The location specific nature of the model also allows for the use of more detailed terrain, weather and fuels input data, producing small errors in smoke movement predictions and thus increased reliability in impact assessments.

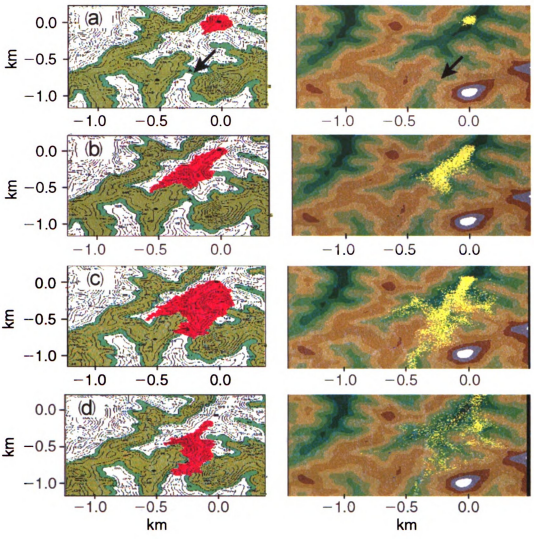

Figure 2.3 Image analysis (left) of smoke plume on night of March 20, 1997 and PB-Piedmont simulated smoke (right) at (a) 2150 LST, (b) 2215 LST, (c) 2255 LST and (d) 2354 LST (modified from Achtemeier, 2006; pg. 92).

While progress is continually made in smoke dispersion and fire effect modeling, there are still short-comings that need to be addressed. First and foremost, many smoke dispersion models were created based on typical industrial point sources, such as smokestacks (McGrattan 2003). Because the energy output and plume rise are smaller

for industrial sources than for wildland fires, the governing equations need to be modified for modeling high intensity wildfires. Also, as Miranda (2004) points out, smoke dispersion depends on the emission of pollutants to the atmosphere, which is highly dependent upon fire progression and characteristics. To account for this dependency there needs to be more emphasis on integration between smoke and fire progression models, taking into account wind field distribution (both horizontal and vertical), the advance of the fire line and the interaction between the fire and wind (Miranda 2004). To try to account for these interactions, several attempts have been made to create modeling *systems* that incorporate different aspects of the fire and the fire environment in attempts to better predict aerosol concentrations and reduced visibility.

The integration of four simulation models was discussed by McKenzie *et al* (2006). In their study, a Fire Scenario Builder (FSB), which creates scenarios of fire starts, sizes and locations, was combined with a meteorological model (in this case the PSU/NCAR Mesoscale Model, MM5), an emissions production model (EPM) and a dispersion model (CALPUFF) to simulate the contribution of wildfires to elevated $PM_{2.5}$ concentrations and reduced visibility (Figure 2.4) (McKenzie et al. 2006). 24 hr mean $PM_{2.5}$ concentrations and light extinction coefficients were calculated. Results of this study showed that while the system did accurately predict the 20 worst days of reduced visibility, it underestimated those daily averages of $PM_{2.5}$ concentrations. The system was also not able to predict the most extreme event, largely due to the fact that wildfires were most likely not the only source of regional haze during this time. These limitations within the modeling system need to be addressed and improvements need to be implemented in the FSB, to better simulate the total number and size of simulated fires.

Changes in vegetation cover over time need to be incorporated into the system as well, allowing for modification of the fuel layers, which influences potential and actual biomass consumed and smoke produced from the emissions simulator (McKenzie et al. 2006).

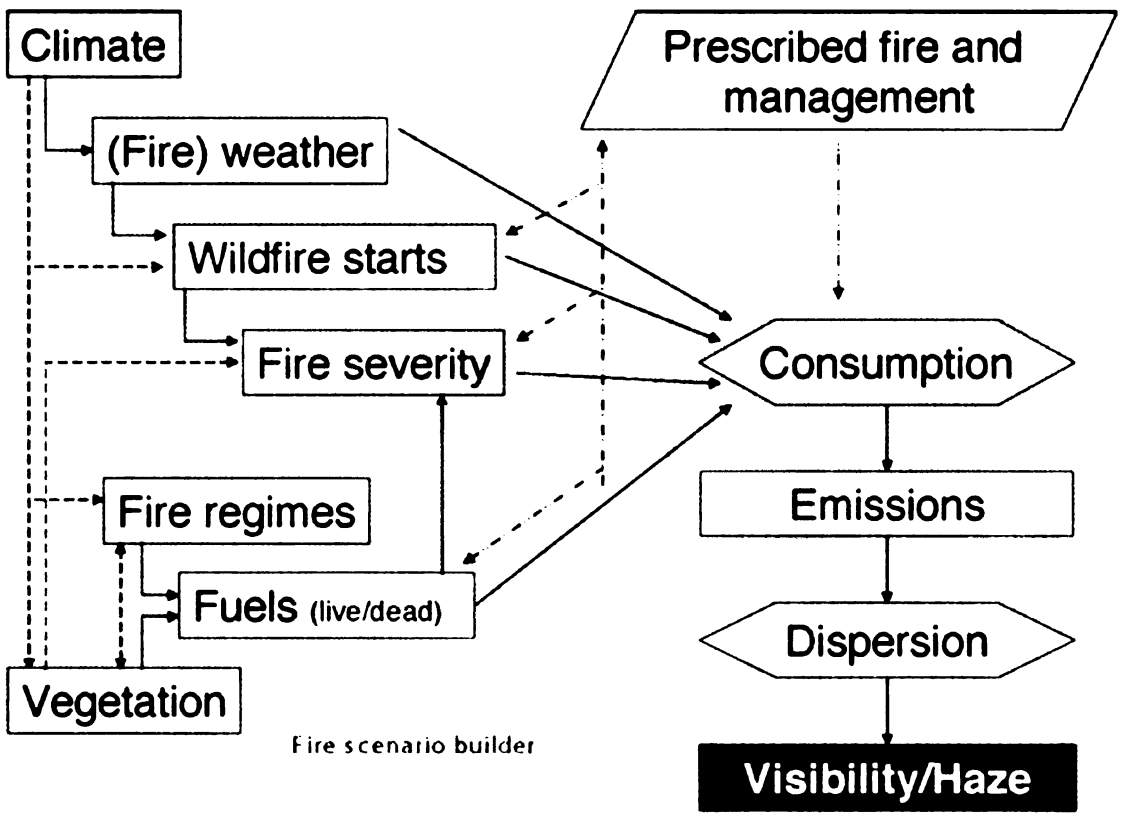

Figure 2.4 Schematic of modeling framework. Dotted arrows indicate interactions which are turned off or for which default values are assumed (from McKenzie *et al*, 2006; pg 281).

Valente *et al* (2007) describes another integration system that combines DISPERFIRE (Miranda, Borrego, and Viegas 1994) and FireStation (Lopes, Cruz, and

Viegas 2002). DISPERFIRE is a real-time system developed to simulate the atmospheric dispersion of pollutants emitted during a forest fire while FireStation is a software system aimed at the simulation of fire spread over complex topography (Valente et al. 2007). Input data for DISPERFIRE (topography, wind speed, wind direction, ignition time, fire rate of spread and heat released) were estimated by the FireStation software system. Measurements of aerosol pollutants such as PM_{10}, NO, NO_2 and CO were collected at the burn locations to validate the model and compare observed and simulated of aerosol concentrations and smoke dispersion. Results of this study showed that although estimated and measured aerosol concentrations compared relatively well, emission estimates are a large area of uncertainty in this model (as well as other dispersion models).

Another integrated system designed for smoke impact prediction is ClearSky, a numerical smoke dispersion forecast system for agricultural field burning created for smoke management purposes in the Inland Pacific Northwest (Jain et al. 2007). Three components, a web-based field burning scenario generator, the CALPUFF dispersion model, and a web-based application for reviewing CALPUFF animations, are combined with an atmospheric model (PSU/NCAR mesoscale model, MM5 (Grell, Dudhia, and Stauffer 1994)) to create the modeling system. Input information for the simulations is provided by data collected directly by the fire manager. Default parameters allow managers to estimate smoke dispersion and aerosol concentrations when they are unable to submit their specific burn information in enough time for estimates to be generated. While there are four different types of agricultural field burning (head fire, mass ignition, strip head fire and backing fire) ClearSky models the field burns as head fires (Jain et al.

2007). An evaluation of the model by Jain *et al* (2007) shows that ClearSky is able to successfully predict where and by how much agricultural burning increased aerosol concentrations (Figure 2.5) on days when the MM5 predicted meteorology is in agreement with observed meteorology.

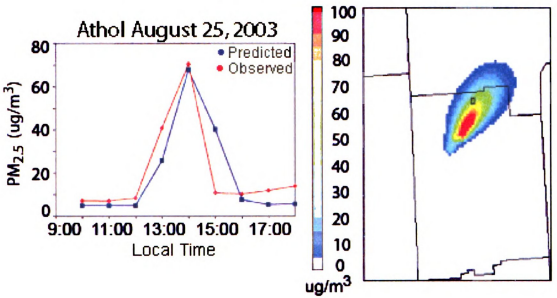

Figure 2.5 Observed and predicted $PM_{2.5}$ concentrations (left) a monitoring site in Idaho and the corresponding predicted plume concentration contours (right) during August 25, 2006 (modified from Jain *et al*, 2007; pg. 6756).

On these days, the maximum modeled concentrations at the observing sites were approximately the same as observed maximum concentrations, allowing the fire manager to have confidence in the model results and in their 'burn'/'no-burn' decision. While ClearSky simulations were in good agreement when the simulated meteorological conditions were satisfactory, large discrepancies occurred in PM concentrations and timing when the simulated meteorological conditions were not in good agreement with

the observations. This suggests that the modeling framework is highly dependent on the meteorological forecasts. Jain *et al* (2007) suggest using ensemble meteorological forecasts or nested, higher resolution domains, particularly in areas with complex terrain. While more efforts are needed to assess ClearSky in varying situations, it shows promise in evaluating and estimating smoke and aerosol impacts. ClearSky's usefulness in simulating smoke impacts from agricultural fires initiated the creation of BlueSky, a framework designed to predict smoke impacts from not only agricultural burns, but from forest and range fires as well.

The BlueSky Smoke Modeling Framework

The BlueSky Smoke Modeling framework is a smoke forecasting system that provides daily predictions of surface smoke concentrations from prescribed fire, wildfire and agricultural burn activities (O'Neill, Ferguson, and Peterson 2003). BlueSky is a modular component system comprised of the following basic elements: source characteristics, emissions models, weather models, and smoke dispersion models. The modular system of BlueSky eliminates the need for large amounts of user inputs and provides immediate web-based feedback, showing cumulative impacts of smoke from biomass burning (Ferguson, Peterson, and Acheson 2001; O'Neill et al. 2005).

As discussed above, smoke dispersion models, though available for years, have been hindered by being too complicated for operational use or too simple to be considered realistic. The USDA Forest Service with cooperation from the US Environmental Protection Agency (EPA) worked together with fire managers and air quality regulators to create the BlueSky modeling system that is both realistic and user

friendly. Since its inception for operational modeling of wildfire smokes in 2002 (Berg et al. 2003), written documentation regarding the BlueSky Smoke Modeling Framework has been limited to mainly conference proceedings and short technical notes.

There are many advantages to the BlueSky's modular framework. The system can be utilized in a wide array of applications as unnecessary model components for a particular application can be easily turned on and off (Larkin et al. 2007). Sestak *et al* (2002) notes that because BlueSky relies strongly on real-time fuels and weather information, it can provide realistic and accurate estimations of smoke dispersion throughout a region. The ability to use information concerning all fire activity in a region allows BlueSky to not only predict smoke impacts from a single fire but also the cumulative impacts from multiple fires, further increasing its applicability to air resource management (BSRW 2006).

In 2003, BlueSky was integrated with the EPA's Rapid Access INformation System (RAINS) which is a Geographical Information System (GIS) useful for visual displays of geographical data. The combined system is called BlueSkyRAINS. The integration of these two products allows users to zoom in on areas of interest, step through time, and overlay other GIS layers (geopolitical boundaries, meteorological fields, topography, etc) in order to interactively view mapped geographic information and analyze the potential smoke impacts more completely (O'Neill, Ferguson, and Peterson 2003; O'Neill et al. 2005).

BlueSky's deterministic approach of using physical laws to determine the direction and speed of smoke movement across a landscape allows it to be used for multiple applications (Potter, Larkin, and Nikolov 2006). It is most often used by smoke

and fire managers to assess smoke impacts due to prescribed burn activities, wildfires and wildland fire use fires (BSRW 2006; Adkins et al. 2003). The goal of BlueSky is to help minimize smoke impacts on local and regional environments. BlueSky has proven to be a valuable communication tool. It provides regional forecasts of smoke impacts that can be used to issue public safety notifications and inform the public in those regions to be cautious when driving or being outdoors as smoke may be reducing visibility and/or air quality (Berg et al. 2003; Evers 2006). If a community was "smoked out" or heavily impacted by high amounts of smoke, BlueSky can be a useful post-smoke event research tool to assess the situation and evaluate if that situation could have been predicted and/or prevented (O'Neill et al. 2005).

The ability of BlueSky to predict timing and location of smoke impacts as well as surface concentrations of PM as a result of wildfires has been tested in a small number of case studies. Wildfires used as test cases include: the Quartz Complex Fire of 2002 (O'Neill, Ferguson, and Peterson 2003; Evers et al. 2006), the Hayman Fire and Bitterroot Complex of 2002 (Adkins et al. 2003; Rapp 2006), the Rex Creek wildfire of 2001 (Berg et al. 2003), the Frank Church Complex of 2005 (Larkin et al. 2007), the Black Range Complex of 2005 (BSRW 2006) and a series of wildfires across northern California in 2006 (Fusina et al. 2007). BlueSky was consistently found to accurately predict the smoke plume trajectory and timing of smoke impacts seen in the observations. These studies also showed that while simulated surface $PM_{2.5}$ concentrations were significantly lower than observed concentrations, BlueSky was able to predict the maximum, cumulative concentration over an entire domain. The previous case studies suggest that

while BlueSky is a useful tool that integrates fire occurrence, fuels and meteorological data form multiple fires, there is still a need to improve its performance.

Uncertainty and limitations within the BlueSky framework include: errors in real-time fire characteristics data due to lack of consistent and reliable reporting systems and the migration of wildfires through varying complex fuel load and fuel conditions (Ferguson, Peterson, and Acheson 2001); lack of operational monitoring networks to compare with simulated data (BSRW 2006); and high sensitivity of the model to predicted wind directions that may lead to small errors in timing and location of simulated smoke plumes to severe underestimates in PM concentrations at a particular location (Berg et al. 2003). Most importantly, the accuracy of the input data is vital to the accuracy of BlueSky predictions of smoke impacts as inaccuracies within the input data will propagate through the entire system (Larkin et al. 2007). Larkin *et al* (2007) also suggests that while BlueSky simulates wildfires as a single, large convective plume, in reality wildfires are comprised of multiple convective plumes and this could be reason for the underestimates in surface emissions. In the study, the Rex Creek fire was simulated as one single convective plume and also as 5 and 10 smaller convective plumes. Results showed that while increasing the number of convective plumes substantially increases the near-surface $PM_{2.5}$ concentration estimates (Figure 2.6), it also shows less variability and higher than observed averages. Liu *et al* (2006) found similar results, splitting the fire into several component fires increased the surface concentrations of $PM_{2.5}$, which suggests that knowledge of the fire behavior, and thus accurately simulating wildfires, is important to accurately estimate smoke impacts (Larkin et al. 2007).

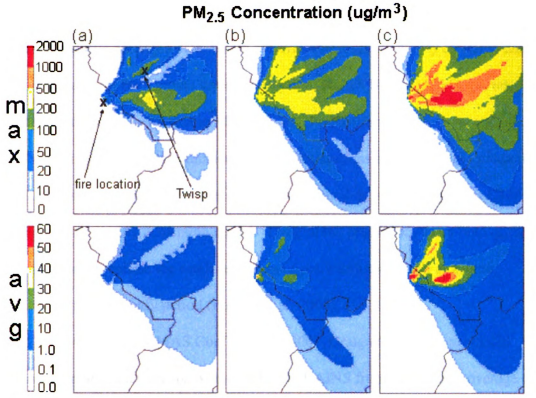

Figure 2.6 Maximum average and ground concentrations for the Rex Creek wildfire for the period of August 19-26, 2006 when the fire is (a) treated as a single fire, (b) split into 5 fires and (c) split into 10 fires. In all cases the total area burned is the same (modified from Larkin *et al*, 2007).

With some success of the BlueSky system, researchers have focused on the integration and expansion of BlueSky with other operational systems to further increase the smoke impact assessment potential. Pouliot *et al* (2005) integrated BlueSky and the Sparse Matrix Operator Kernel Emission (SMOKE) processing system to produce higher resolution smoke estimates for use in regional-scale chemical transport models such as the Community Multi-scale Air Quality (CMAQ) model. SMOKE is a tool that creates gridded, speciated, and temporally allocated emissions estimates for use in atmospheric chemistry models (Pouliot et al. 2005), and can convert the resolution of the emission

data to that needed by an air quality model (in this case CMAQ). For example, SMOKE can convert wildfire emission data, which are available daily, to hourly emission data for each grid cell and for each model layer. This system (called BlueSky-EM) was tested for wildfires that occurred in Florida in May of 2001. Preliminary results show a good correlation between BlueSky estimated $PM_{2.5}$ concentrations and those same predictions by the CMAQ simulations. The agreement between models is encouraging as CMAQ is a widely used air quality dispersion model. The graphic predictions from both of these models also closely mimic the satellite images of the wildfires as well as plume movement during the study period (Pouliot et al. 2005).

At the 6th Annual CMAS Conference in 2007, Craig *et al* (2007) presented preliminary findings on the expansion of BlueSkyRAINS from its limited coverage over the western U.S. to national coverage over the contiguous United States (called BlueSky-N). According to Craig *et al* (2007), the expansion of BlueSkyRAINS can be used for preparation of a national emissions inventory of $PM_{2.5}$ due to anthropogenic, biogenic and fire emissions. Existing satellite technologies and remote sensing are being combined to help expand the applications of BlueSky-N and create a uniform method of determining fire sizes and locations, so that the fire contribution can be more accurately determined. This national emissions inventory will provide a 36 km resolution national forecast of ground level $PM_{2.5}$ concentrations (Craig et al. 2007). Consistent with previous findings, preliminary results presented showed that the BlueSky-N system was able to predict the timing and transient nature of the smoke plume but under-predicts the peak magnitude of surface $PM_{2.5}$ concentrations.

As BSRW (2006) concluded, the BlueSky system is reliably the "best modeling framework available for wildland fire smoke predictions at this time, but it is still is a research tool and needs further development". As indicated previously, attempts have been made at model evaluation and improvement, but research is still necessary as model enhancements become integrated and operational in the BlueSky system. Studies evaluating BlueSky predictions have not been done on large wildfires and currently there is still uncertainty concerning all the system components. Rather than just looking at the entire BlueSky framework as a whole, studies concerning individual system components are necessary for understanding the error sources for BlueSky predictions.

Model Description

$PM_{2.5}$ Concentrations and Smoke Trajectory Simulations

The BlueSky Smoke Modeling framework produces predictions of smoke plume trajectories and $PM_{2.5}$ concentrations. The BlueSky framework is a system that combines meteorology and emissions to produce a regional-scale analysis of aerosol concentrations and smoke dispersion. The major components of BlueSky are fire characteristics, meteorology, emissions and smoke dispersion (Figure 2.7). Of those, only fire characteristics and meteorology are required as inputs for the running of BlueSky, while all other variables are derived within the framework.

Hourly, four-dimensional (x,y,z,t) gridded data is needed for the dispersion and trajectory models within BlueSky (Larkin et al. 2007). Although different meteorological

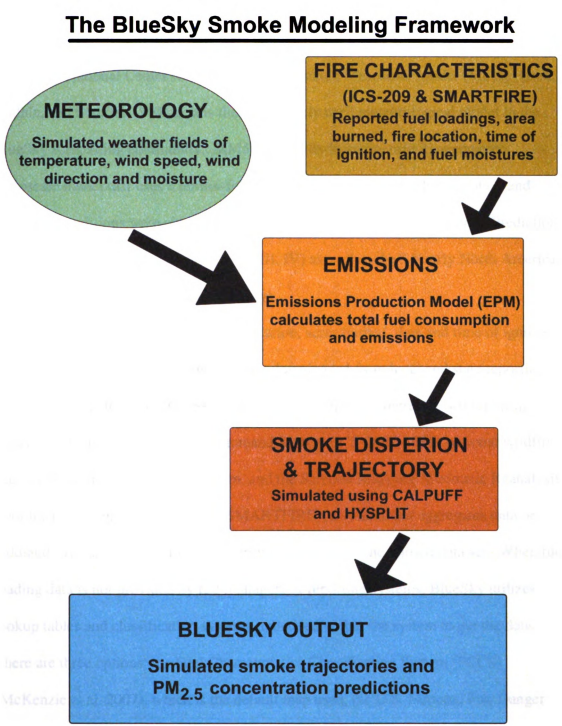

Figure 2.7 Components of the BlueSky modeling system.

models can be used to estimate meteorological inputs for BlueSky, the meteorological predictions presented in this thesis were simulated using the Pennsylvania State University/National Center for Atmospheric Research Mesoscale Model (MM5) (Grell, Dudhia, and Stauffer 1994) as it is the most widely used meteorological model in the BlueSky forecasting community. MM5 is a non-hydrostatic, primitive equation mesoscale model that uses a terrain-following coordinate system. Initialization and boundary conditions were obtained using National Center for Environmental Prediction (NCEP) 6-hourly Eta model output (Part III, IV) as well as the 3-hourly North American Regional Reanalysis (NARR; Part IV only).

Fire characteristics such as fire location, acres burned, date and time of ignition, fuel loading and fuel moisture information downloaded from local and state reporting systems and inputted into BlueSky. Currently for wildfires, there are two reporting systems being used: the Incident Command System (ICS-209), a U.S. national wildfire and wildland fire use reporting system, and the Satellite Mapping Automatic Reanalysis Tool for Fire Event Reconciliation (SMARTFIRE), a system that aggregates data on wildland fire size and location from various sources into one unified data set. When fuel loading data is not provided by fire managers or reporting systems, BlueSky utilizes lookup tables and classification systems imbedded within the system to get the data. There are three options: the Fuel Characteristics Classification System (FCCS) (McKenzie et al. 2007), which is the default map used, the U.S. National Fire Danger Rating System (NFDRS) (Cohen and Deeming 1985) and the revision to the NFDRS by Hardy *et al* (1998) over the 11 western U.S. states. All three classification systems have a 1 km grid spacing.

Fire characteristics, are then inputted into the Emission Production Model (EPM; (Sandberg and Peterson 1984) to calculate total fuel consumption and emissions. Total fuel consumption is first calculated and then a time profile is used to allocate the emissions diurnally (Larkin et al. 2007). Wildfire time profiles are based upon the Western Regional Air Partnerships profile (WRAP and WGA 2005), the percent of total area burned per hour is given in Table 2.1.

Table 2.1 Temporal allocation of acres burned in a day for wildfires. Data developed by the Western Regional Air Partnership (from WGA/WRAP, 2005).

Hour	Percent
0-9	0.57
10	2.00
11	4.00
12	7.00
13	10.00
14	13.00
15	16.00
16	17.00
17	12.00
18	7.00
19	4.00
20-23	0.57

Emission dispersion is calculated using CALPUFF (Scire, Strimaitis, and Yamartino 2000). CALPUFF is a puff dispersion model that simulates point, volume or area sources (assuming that the plume dispersion is Gaussian). A pre-processing program, EPM2BAEM, is used to convert EPM output to the proper format for use in CALPUFF. CALMET, a diagnostic meteorological model that calculates the three

dimensional winds and temperatures, as well as microphysical parameters such as surface characteristics, dispersion parameters and mixing heights (Scire et al. 2000), is used to convert the MM5 estimations into a mass-conserving field for use in CALPUFF. Smoke trajectories are simulated using the Lagrangian particle model, HYSPLIT (Draxler and Hess 1997). Trajectories are initiated at a height of 10 m and thus do not account for initial buoyancy effects due to the heat given off by a fire. The final products created by BlueSky are visual images of smoke plume trajectories and shape, as well as surface aerosol concentrations such as $PM_{2.5}$.

Summary

Part II provided background information on smoke dispersion modeling as well as the BlueSky smoke modeling framework. A literature review of each area was presented highlighting major limitations of smoke dispersion modeling and evaluation studies conducted using the BlueSky framework. A discussion of the BlueSky model setup was also given. The following chapters present the results of two case studies used to evaluate BlueSky's ability in predicting smoke plume trajectories and surface concentration distributions of $PM_{2.5}$.

PART III

NORTHERN CALIFORNIA, AUGUST 2006

Introduction

The total number of acres burned in the 2006 and 2007 wildland fire seasons were over 200% of the ten year average (NIFC 2008). Although the number of wildfires has been decreasing since the 1980's, the sizes of wildfires have been steadily increasing, with nearly 10 million acres burned in just over 96,000 individual wildfires in 2006 and 9.3 million acres burned in over 85,000 wildfires in 2007 (NIFC). The number of acres treated by prescribed fires also increased in 2006 and 2007 to more than 9.8 and 9.3 million acres, respectively (up from 8.6 million acres in 2005) (NCDC 2008). Wildland fires are a necessary component of the forest ecosystem as well as an important tool for fuels management practices. But as wildland fires continue to increase in size, increased smoke emissions can cause problems related to air quality standards and visibility.

While numerous atmospheric dispersion models have been developed for predicting the transport and dispersion of atmospheric pollutants (Scire, Strimaitis, and Yamartino 2000; Binkowski and Roselle 2003; Bacon et al. 2000), few have been designed specifically to simulate smoke from wildland fires. To provide a tool for simulating smoke transport and dispersion from wildland fires, a smoke modeling framework called BlueSky was developed by the USDA Forest Service AirFire Team in early 2000 and became operational in parts of the Pacific Northwest by 2002 (Berg et al. 2003). This modeling framework, initially designed for prescribed burn decision support, integrates consumption, emissions, meteorology, and dispersion models to predict smoke trajectories and concentrations of particulate matter. BlueSky smoke predictions are

available daily across the contiguous U.S. and the output has been used by air regulators, burn bosses and smoke managers as a guide to help make 'go' and 'no-go' decisions about prescribed fires and the subsequent burn plans. Since its inception, BlueSky has evolved to be a useful tool in wildfire monitoring as well, especially in the West where the risk of large wildfires is greater. BlueSky can help to track day-to-day emissions and plan suppression strategies. BlueSky is becoming a "one-stop shop" for regional smoke concentration and emissions tracking across all land ownership. While used widely, BlueSky's output has not been rigorously validated against field observations, and the accuracy of its predictions are uncertain under different meteorological conditions. To date, validation efforts of BlueSky's ability to simulate wildfires have been limited to isolated cases in the Northwest (Adkins et al. 2003; Berg et al. 2003; Larkin et al. 2007; BSRW 2006) and Southeast (Pouliot et al. 2005; Craig et al. 2007).

Although none of the existing validation efforts have been subjected to peer review, the studies listed above have produced similar results. In a study focused on the 2002 Hayman Fire in Colorado, Adkins *et al.* (2003) found the location and timing of predicted smoke impacts to agree with observations while the predicted $PM_{2.5}$ concentrations were orders of magnitudes smaller than observations. Larkin *et al.* (2006) conducted a similar study using data collected during the 2001 Rex Creek Wildfire in Washington and the 2005 Frank Church Wildfire in Idaho. The comparisons between smoke plume trajectories and shapes were found to agree quite well with satellite images of significant observed smoke concentrations, but, BlueSky failed to accurately predict the observed magnitudes of $PM_{2.5}$ concentrations.

Additional case studies in different geographical regions are needed to further assess the accuracy of BlueSky and to document the strength and weakness of the modeling system. In an effort to provide better information pertaining to fire weather and smoke dispersion/transport, the California and Nevada Smoke and Air Committee (CANSAC) has been running a BlueSky smoke prediction system in real-time for the state of California and Nevada. In this paper, we describe results from an effort to validate the CANSAC BlueSky smoke predictions as part of a project funded by the Joint Fire Science Program to develop tools for estimating contributions of wildland and prescribed fires to air quality in the Sierra Nevada mountains. Surface in-situ observations and remotely sensed imagery are used in comparison with model output to assess the accuracy of the BlueSky modeling framework in predicting $PM_{2.5}$ concentrations and smoke plume trajectories.

Methods

Study Area

Northern California is a region of contrasting landscapes and diverse topography (Figure 3.1). Northern California is bordered to the west by the Cascade Range and the Klamath and Siskiyou Mountains. The Klamath and Siskiyou mountains range in elevation from around 6,000 ft (1829 m) to 8,000 ft (2438 m) above the mean sea level (MSL). These mountainous regions are forest covered and their small ranges are separated by deep canyons. The Cascade Mountains were formed by volcanoes and, in California, elevations range from about 4,500 ft (1372 m) to 5,000 ft (1524 m) MSL.

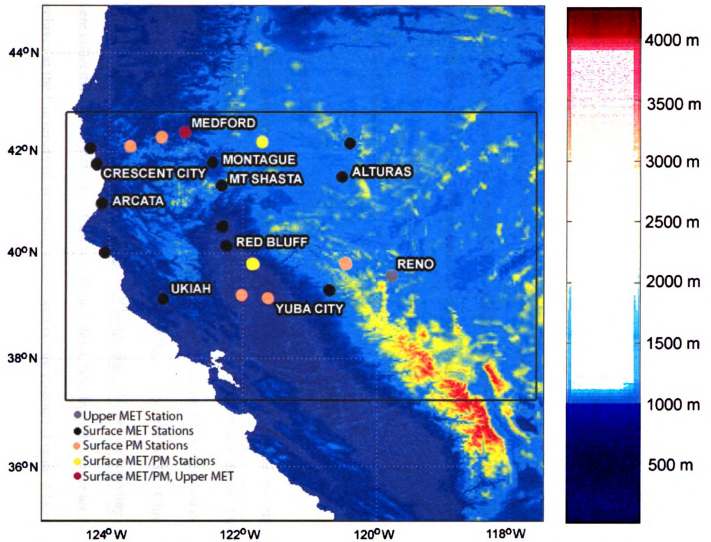

Figure 3.1. Terrain map of northern California and southern Oregon, including locations of observational meteorological and $PM_{2.5}$ stations. The black box indicates the simulated 4km domain.

To the east, northern California is defined by a basin and range province, which extends into Oregon and Nevada. California experiences a variable climate with two main seasons, one rainy and one dry. In northern California, the rainy season occurs during the months of October through April, leaving the summer months comparatively hot and dry. Foliage throughout the western area of this region is a conglomerate of mixed evergreen forests, including Douglas, White and Red Fir, and Ponderosa Pine. To the east the vegetation becomes a mixture of chaparral, California prairie, mixed chaparral and a valley needlegrass series. Dry conditions, available fuels and high air temperatures during the dry season make this area ideal for wildfire outbreaks. During the period of study, August 20 – 31, 2006, a series of major wildfires ignited across northern California and southern Oregon.

Observational Data

Hourly surface meteorological data were collected for fifteen stations within the region to evaluate how well the simulated meteorology matches observations. The locations of these stations are shown in Figure 3.1, while Table 3.1 lists each station's geographic information. Observational data were collected from the NCDC Climate Data Online website, http://cdo.ncdc.noaa.gov/CDO/dataproduct. Upper air sounding data were collected for two stations, Medford, OR and Reno, NV, from the upper air data archives at the University of Wyoming (http://weather.uwyo.edu/) (Figure 3.1). $PM_{2.5}$ (particulate matter with diameter less than 2.5 μm) observational data were collected for eight stations within the region (Figure 3.1). Four stations are situated in Oregon near the California border and are useful in capturing the north-northeasterly

transport of fire smoke. The $PM_{2.5}$ data for these stations was collected from the Oregon Department of Environmental Quality (DEQ). To obtain hourly visibility data, the Oregon DEQ collects Beta Scattering Units (BSCAT) which are collocated with 24 hour average $PM_{2.5}$ filters. A linear regression is used with the data from the collocated monitors and the "correlation" equation is applied to the hourly visibility data to obtain hourly $PM_{2.5}$ estimates. The other four $PM_{2.5}$ monitoring stations are found within the northern California region. Data for those stations came from the California Air Resources Board (CARB) Aerometric Data Analysis Management (ADAM) system database. Hourly $PM_{2.5}$ values for these stations were sampled by Met One Beta Attenuation Monitors (BAM).

Satellite Observations

BlueSky not only outputs hourly surface concentrations of $PM_{2.5}$ but also graphical images showing smoke plume shape and trajectory. To qualitatively assess the accuracy of smoke plume shape and trajectory, images from the Moderate Resolution Imaging Spectrometer (MODIS) Satellite Fire Detection website Hazard Mapping System (HMS) are used. These images are quality controlled displays of fires and significant smoke plumes as detected by meteorological satellites (McNamara et al. 2004). While HMS is a useful and advanced tool for identifying smoke plumes, there are limitations that should be considered when using this imagery. First, there is no way to discriminate between agricultural or controlled burns and wildfires. This discrimination can be done if the duration of a fire is known as wildfires usually last longer than agricultural or controlled fires. Second, small fires that are not producing large amounts

of heat or fires burning below a thick canopy overgrowth may go undetected because they cannot be seen or they blend in with the hot background due to high surface temperatures and reflectivity (this is especially prominent in the western US summers). Also, the satellites themselves can be a limitation. Satellites (using the 3.9 micron band) are not able to see through clouds other than cirrus and in the middle of the day and when the sun angle is high, smoke is hard to detect because satellites have a hard time distinguishing the differences between high levels of reflectivity and smoke (McNamara et al. 2004). Despite these limitations, the HMS is still a very useful imagery database for qualitative smoke plume comparisons. MODIS aerosol optical depth data images are used to quantitatively compare the concentrations of aerosols within BlueSky predicted smoke plumes to observed concentrations.

Table 3.1. Geographic station information for meteorological and $PM_{2.5}$ observations[ab]

	Site ID	Name	State	Latitude	Longitude	Elevation	Type	Network
1	72595724215	MOUNT SHASTA	CA	41.333	-122.333	1078	S	NCDC
2	72595899999	ALTURAS	CA	41.5	-120.533	1341	S	NCDC
3	72497399999	CHICO MUNICIPAL	CA	39.8	-121.85	73	S	NCDC
4	60070002	CHICO MANZANITA AVE	CA	39.8	-121.85	73	P	CA ARB
5	72584523225	BLUE CANYON AP	CA	39.3	-120.717	1609	S	NCDC
6	72584899999	SHELTER COVE	CA	40.017	-124.067	68	S	NCDC
7	72590523275	UKIAH MUNICIPAL AP	CA	39.133	-123.2	189	S	NCDC
8	72591024216	RED BLUFF MUNICIPAL ARPT	CA	40.15	-122.25	106	S	NCDC
9	72592024257	REDDING MUNICIPAL ARPT	CA	40.517	-122.317	153	S	NCDC
10	72594524283	ARCATA AIRPORT	CA	40.983	-124.1	62	S	NCDC
11	72595524259	MONTAGUE SISKIYOU COUNTY AP	CA	41.783	-122.467	803	S	NCDC
12	99401299999	CRESCENT CITY	CA	41.75	-124.183	17	S	NCDC
13	60631009	PORTOLA - 161 NEVADA ST	CA	39.81	-120.47	1500	P	CA ARB
14	60111002	COLUSA	CA	39.2	-122.01	18	P	CA ARB
15	72483899999	YUBA CO	CA	39.13	-121.61	19	S	NCDC
16	61010003	YUBA CITY - ALMOND ST	CA	39.13	-121.61	19	P	CA ARB
17	72597024225	MEDFORD ROGUE VALLEY INTL AP	OR	42.383	-122.867	396	S	NCDC
18	20448	MEDFORD, GRANT AND BELMONT	OR	42.314	-122.879	396	P	OR DEQ
19	72597	MEDFORD/JACKSON	OR	42.38	-122.87	397	U	WW
20	72597699999	LAKEVIEW (AWOS)	OR	42.167	-120.4	1441	S	OR DEQ
21	72589594236	KLAMATH FALLS INTL AP	OR	42.15	-121.717	1245	S	NCDC
22	10120	KLAMATH FALLS - MILLER ISLAND	OR	42.158	121.816	1245	P	OR DEQ
23	72036599999	BROOKING AIRPORT	OR	42.083	-124.283	140	S	OR DEQ
24	21068	ILLINOIS VALLEY	OR	42.1	-123.68	425	P	OR DEQ
25	18432	PROVOLT SEED ORCHARD	OR	42.28	-123.23	358	P	OR DEQ
26	72489	RENO	NV	39.56	-119.77	1516	U	WW

[a]Note type 'S' and 'U' indicate surface and upper air meteorological observations, 'P' indicates $PM_{2.5}$ observations
[b]The 'WW' network indicates the University of Wyoming WeatherWeb online database

Model Simulations

The data described above are used to evaluate the real-time smoke predictions from the operational CANSAC BlueSky runs at the Desert Research Institute. BlueSky has five components that work together to predict surface concentrations and smoke plume trajectories from wildfires and prescribed burns. The five components are meteorology, fuel load, fire behavior, emissions, and smoke dispersion (O'Neill 2003). The meteorological fields are predicted using the Penn State/NCAR fifth generation mesoscale model (Grell, Dudhia, and Stauffer 1994). The model was configured with four nested domains with the outermost domain of 36-km grid spacing covering western United States and eastern Pacific Ocean and the innermost domain of 4-km grid spacing overlaying the state of California and Nevada. Initial and boundary conditions were obtained from the 6 hourly 40-km ETA forecasts from the National Centers for Environmental Prediction (NCEP). To simulate the transport and dispersion of aerosols from smoke emissions, CALPUFF, a multi-layer, multi-species non-steady state Lagrangian puff dispersion model that can simulate the time and space varying pollutant transport, transformation and removal (Scire, Strimaitis, and Yamartino 2000). The necessary fire input, such as fire location, size, date of burn, and ignition time, was obtained from the National Wildfire 209 Situation Reports (ICS-209). Secondary input information (that information which does not need to be entered manually) includes: length of ignition, type of fire (crown, grass, brush), vegetation type, 1hr, 10hr, and 100hr fuel loading, snow melt month, duff depth, and burn site slope (Table 3.2). Hourly $PM_{2.5}$ emissions were computed using Consume/EPM v1.03, and fuel characteristics input to BlueSky were derived from the Fuel Characteristic Classification System (FCCS).

Table 3.2 BlueSky Input Information

Primary Information	
• Location of fire	• Number of acres burned
• Date of burn	
Secondary Information	
• Ignition duration	• Slope of burn site
• Type of fire	• Fuel harvest date
• Fuel loading: 0-0.25, 0.25-1, 1-3 in	• Number of days since last rain
• Fuel loading: 3-9, 9-20, 20 + in	• Duff depth
• 1000 hr fuel moisture	• 10 hr fuel moisture
Tertiary Information	
• Grass and herbs fuel loading	• Rottenwood
• Litter depth	• Shrub fuel loading
• Terrain elevation	• Total PM2.5 emissions (in tons)
• Total PM10 emissions (in tons)	• Total PM emissions (in tons)
• Total CO emissions in (in tons)	• Total CO2 emissions (in tons)
• Total CH4 emissions in (in tons)	• Total non-methane hydrocarbon emissions (in tons)

[c]Note the total emissions are calculated internally in BlueSky

Results and Discussion

Wildland Fires and Synoptic Weather Conditions during the Study Period

Four main fire complexes were burning during August 20 – 31, 2006. The Orleans complex consisted of two fires (Somes and Buck fires) and was located east of Orleans, CA near the Arcata surface meteorological station (Figure 3.1). Bar Complex, comprised of four separate fires, was located northwest of Weaverville, CA, located in Shasta-Trinity National Forest, near Mt Shasta meteorological station (Figure 3.1). The three fires: Uncles, Rush, and Hancock were part of Uncles Complex located approximately 20 miles northeast of Orleans, CA. Finally, Happy Camp was a large

complex that included 15 separate fires located near Happy Camp, CA (Crescent City is the meteorological station located closest to Happy Camp, Figure 3.1). Containment efforts for these fires were hampered by steep and rugged terrain as well as two main active fire behavior periods on August 24-25 and August 30-31. By August 23 Happy Camp was 100% contained, and the extreme fire behavior during this study period occurred only in the Orleans, Bar and Uncles complexes.

Synoptically, at the beginning of the study period, the West was dominated by an 500 hPa upper level ridge with 12-15 m s^{-1} south-southwesterly winds at the 500 hPa level over northern California and southern Oregon (Figure 3.2a). These wind speeds increased steadily to 18-24 m s^{-1} over the next few days as the ridge weakened and a trough developed over the Pacific Northwest. By August 24, a day when many of the fires exhibited active fire behavior the cut-off low over the Pacific Northwest intensified and within 24 hours (Figure 3.2b), northerly 500 hPa winds, around 8-15 m s^{-1} prevailed over northern California. Wind speeds weakened through the next 36 hours as an upper level ridge moved back into the area. 500 hPa southwesterly winds allowed fire fighters to regain control of the fires and substantial containment progress was made. By the end of the study period, as the ridge moved off to the east and a trough moved in from the Northwest, active fire behavior was again observed as 500 hPa wind speeds increased to 21 m s^{-1} and westerly flow was observed over northern California while northwesterly flow was observed over southern Oregon (Figure 3.2c). By the beginning of September, the 500 hPa winds had weakened again and containment efforts were continued. The Orleans complex was 100% contained as of September 3, but the other two complexes continued to smolder for the next few weeks.

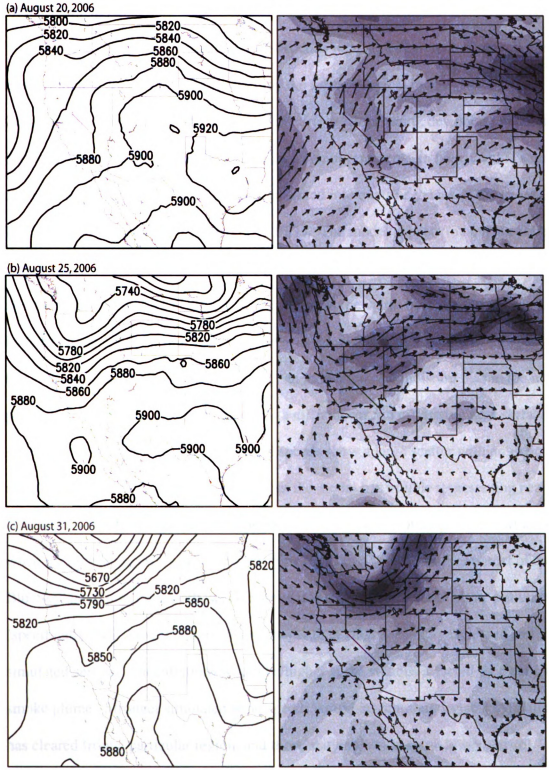

Figure 3.2. Plots of 500 hPa height (left) and wind speed (right) synoptic plots at 12Z (0400 PST). Light shading in the wind speed panels (right) indicates weaker 500 hPa wind speeds while darker shading indicates stronger wind speeds. Contours in the left panel represent 500 hPa isoheights.

Meteorological fields

The accuracy of smoke prediction depends to a large degree on how well the meteorological conditions are simulated by the meteorological model (MM5). Comparison of simulated and observed near surface temperature, dewpoint temperature, and wind speed are shown in Figure 3.3. Each point represents an hourly value across the entire study period. The data points are separated into daytime values (0700 to 1900 PST) and nighttime values (2000 to 0600 PST). The model appears to have a cold bias during daytime and warm bias during nighttime. Generally the model seems to be less accurate when predicting nighttime temperatures as the warm bias at night appears to be larger than the cold bias during the day. Also evident is a higher predicted dewpoint temperatures regardless of the time of day, an indication of a moisture bias in the model prediction. The meteorological model has a difficult time in estimating near surface wind speeds as the comparison with these wind speeds show a large scatter with no in both day and night estimations. While it appears that the model has trouble representing near calm conditions when the observed wind speeds were 0-2 m s^{-1}, it under predicts surface winds when the observed surface winds are stronger (6-10 m s^{-1}). Within the context of the BlueSky modeling framework, weaker simulated wind speeds would allow pollutants (specifically $PM_{2.5}$) to remain in an area longer than what is actually observed and simulated aerosol concentrations would be higher at the stations affected by a particular smoke plume. Stronger simulated wind speeds would inaccurately suggest the pollutant has cleared from a particular region, and those stations would show lower aerosol concentrations.

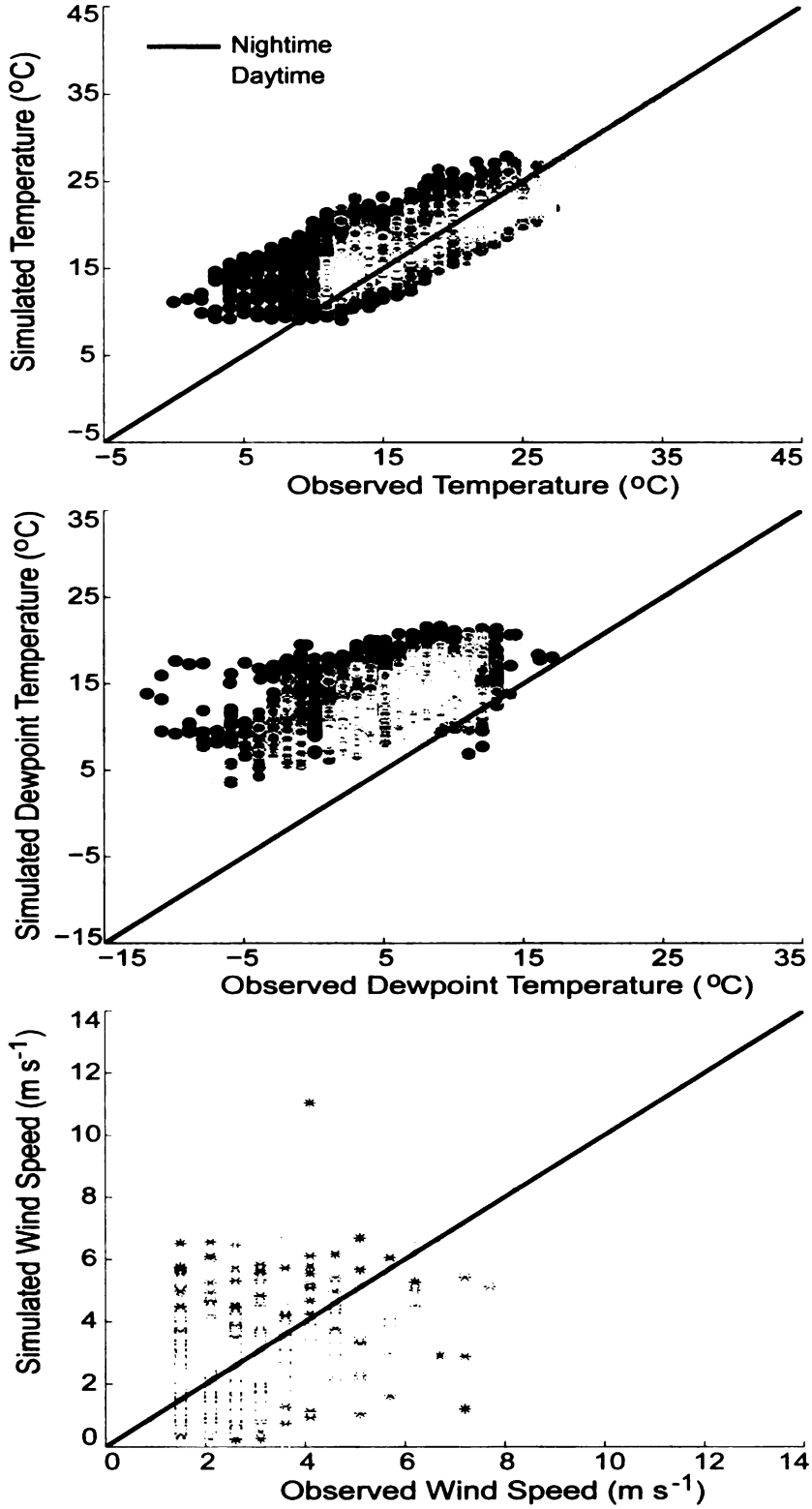

Figure 3.3 Simulated and observed hourly temperature (top), dewpoint temperature (center), and wind speed (bottom) at all fifteen surface meteorological stations used within this study. Gray dots are the day time values while the black dots are night time values.

To evaluate how well the model simulated the diurnal variation of the meteorological fields, time series plots of predicted and observed meteorological variables were produced for all surface meteorological stations. Figure 3.4 shows three stations representing (a) the general pattern represented by the MM5 simulations, (b) the pattern seen along the west coast, and (c) the pattern seen in the northern stations, which are located in steep topography (Figure 3.4c). As Figure 3.4 shows, MM5 was able to capture the day-to-day variations in meteorological conditions due primarily to changes in synoptic conditions. For example, the simulation captured the observed temperature trend with high temperatures at the beginning of the simulation, decreasing temperatures towards the end of the first week, and warming again in the middle of the second week. The model also estimated the transitions between moderate, weak, and strong wind regimes during the study period. Further, the simulation predicted the differences in the diurnal temperature cycle between the inland (Figs. 3.4a and c) and coastal (Figure 3.4b) sites with the latter exhibiting a weaker diurnal signal due to the influence of the ocean, this is true of all the coastal stations used in this study. However the simulated amplitudes of the diurnal temperature cycle are much smaller than observed. It is interesting to note the strong diurnal variation in the observed wind speed with higher winds in the afternoon and lower winds at night. This is due to daytime coupling of the surface winds aloft by turbulent mixing, allowing stronger winds aloft to mix downwards into the surface layer. At night the formation of a surface-based inversion decouples the

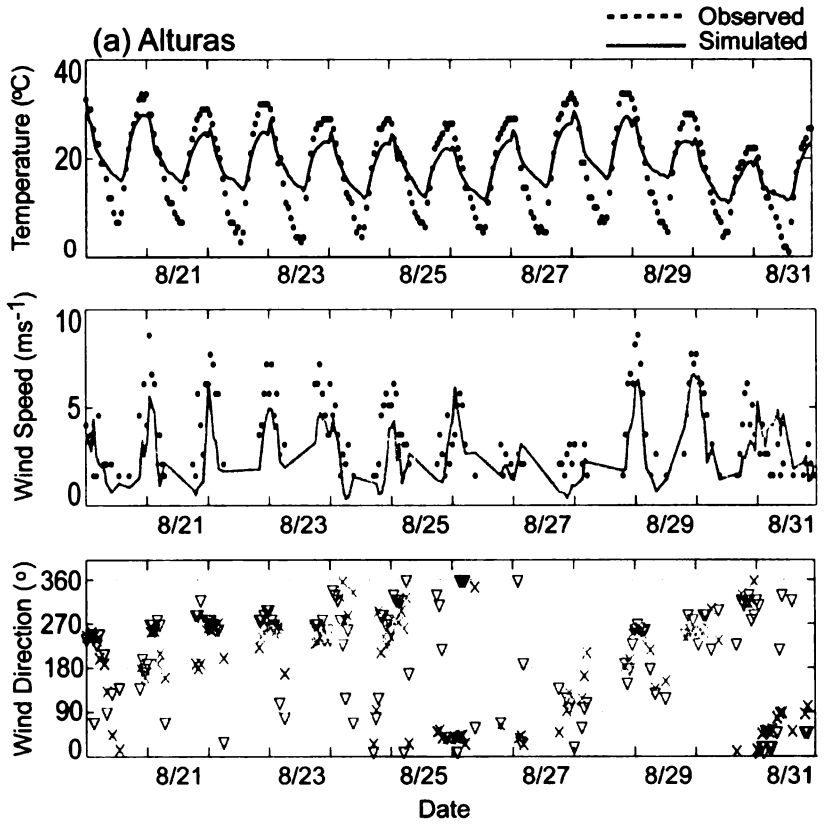
(a) Alturas
Observed
Simulated
Temperature (ºC)
40
20
0
8/21
8/23
8/25
8/27
8/29
8/31
Wind Speed (ms-1)
10
5
0
Wind Direction (°)
360
270
180
90
0
Date

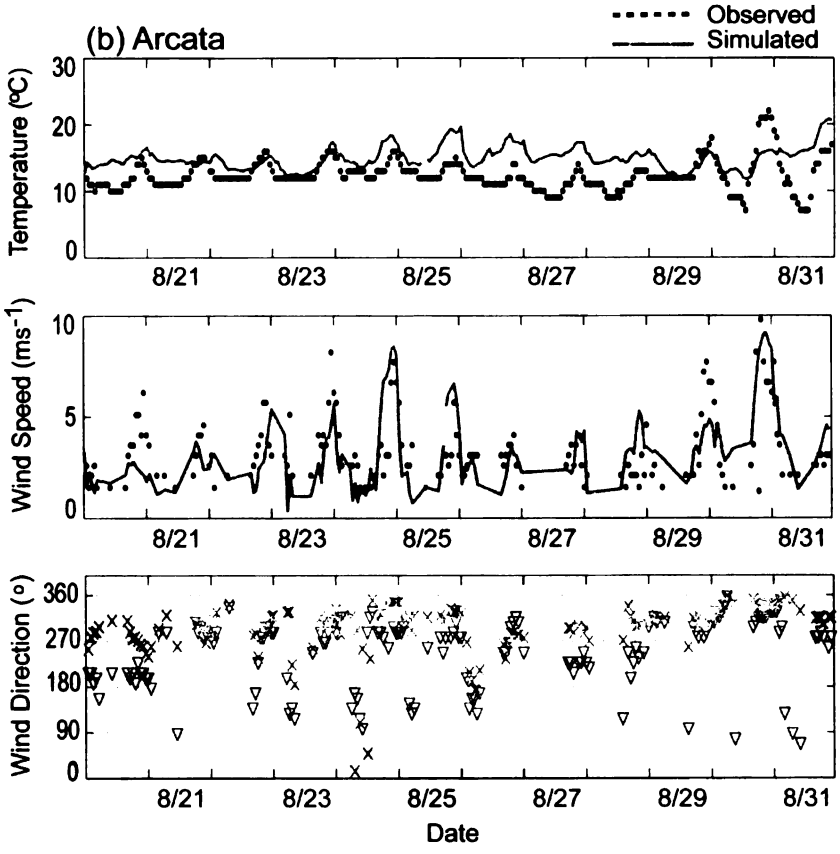
(b) Arcata
Observed
Simulated
Temperature (ºC)
30
20
10
0
8/21
8/23
8/25
8/27
8/29
8/31
Wind Speed (ms-1)
10
5
0
Wind Direction (°)
360
270
180
90
0
Date

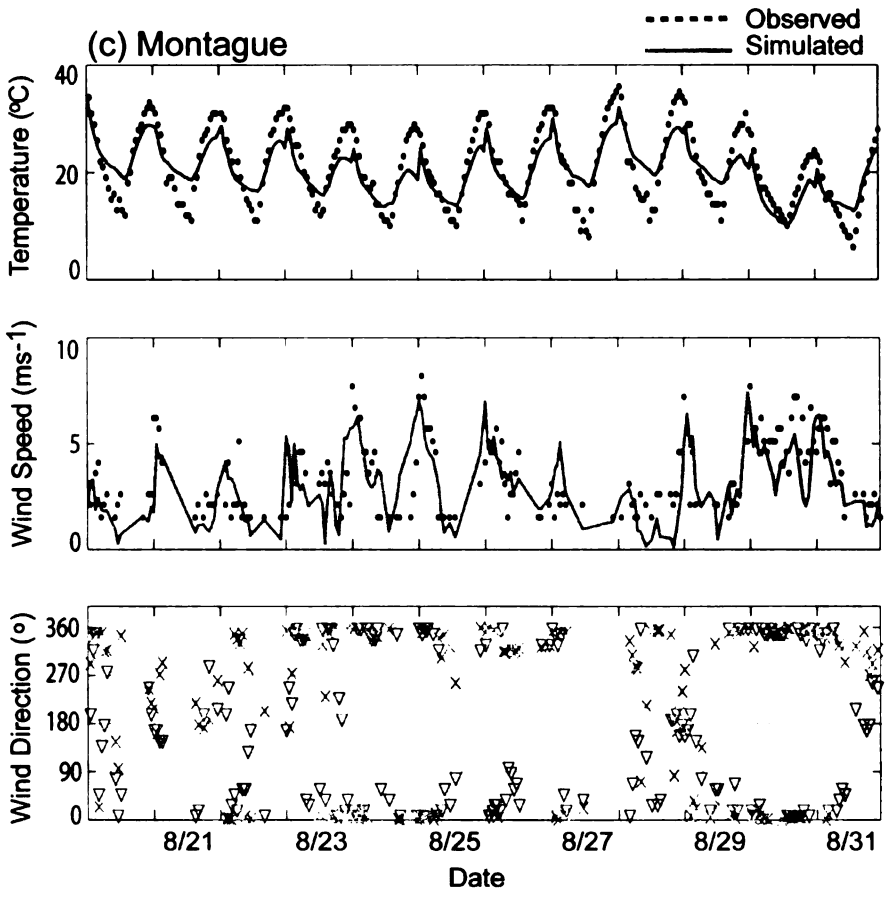

Figure 3.4. Time series plots of surface temperature, wind speed and wind direction at three locations which show (a) the typical MM5 simulated pattern, (b) the pattern observed at stations located along the west coast, and (c) the pattern seen in the northern stations located in diverse terrain. Black dotted lines and upside down triangles (in wind direction time series) represent the observations while gray lines and x's (in wind direction) represent MM5 simulated surface meteorological conditions.

surface layer from the layer above. The simulation reproduced this diurnal variation of wind speed at all locations, although the agreement between simulated and observed wind speed is better at coastal sites (represented by Figure 3.4b) than at inland and higher elevation sites (Figure 3.4a and 3.4c). The difference between stations is most likely due to the less complex topography in the coastal region. The predicted wind direction agrees quite well with the in-situ observations.

Table 3.3 summarizes statistics (mean, RMSE, bias, correlation and error standard deviation) comparing the model with observations to help quantify the errors of the simulation. Simulated errors can be either systematic or random. Systematic errors are errors due to biases within the estimations and if known can be reduced through the use of calibration. Examples of systematic errors are misrepresentation of topography, land use properties and radiation. Random errors on the other hand are due to uncertainty. These types of errors can be reduced through statistical analysis. Examples of random errors are uncertainty within the observations themselves or the initial and boundary conditions used by a model.

Simulated standard deviations (STD) of temperature and dewpoint are smaller than observed, indicating (as mentioned previously) that the model does not estimate the full extent of the temporal variations as seen in the observations. However, the model does do a better job at capturing the variations in wind speed as the STD between simulations and observations are comparable. Linear correlation coefficients (r) show strong correlations between simulated and observed temperatures while weak correlations are apparent between dewpoint temperatures and wind speed. Bias is calculated by subtracting MM5 simulated temperatures, mixing ratios and wind speeds from observations. These values are then summed and then divided by the total number of observations to obtain an average. Day and nighttime temperature bias further illustrate what was seen in Figure 4.5, a warm bias at night, 2.819 °C and a daytime cool bias of -1.492°C. Mixing ratio bias indicates a large moist bias, ranging from 8.340 g kg^{-1} at night and 6.110 g kg^{-1} during the day. Wind speed bias is negative during the entire day, in agreement with scatter plots results, MM5 simulated near-surface wind speeds are

Table 3.3 Meteorological comparison statistics for surface temperature, mixing ratio and wind speed[c]

		Temperature (°C)			Dewpoint Temperature (°C)			Wind Speed (m s^{-1})		
	Statistics	Night	Day	All	Night	Day	All	Night	Day	All
Number of data points		1656	1972	3628	1533	1783	3315	770	1610	2380
OBSERVATIONS	Mean	14.01	23.35	19.09	5.45	6.53	6.03	2.55	3.63	3.28
	STD	2.17	2.65	2.76	2.22	2.09	2.16	1.08	1.32	1.29
MM5	Mean	16.83	21.86	19.56	13.80	12.64	13.17	2.51	3.03	2.86
	STD	1.95	2.23	2.29	1.77	1.86	1.83	1.20	1.28	1.26
	Bias	2.81	-1.49	0.47	8.34	6.1	7.14	-0.04	-0.59	-0.41
	r	0.665	0.890	0.864	0.366	0.600	0.457	0.35	0.504	0.487
	Error STD	3.59	3.37	4.08	4.81	3.60	4.34	1.51	1.70	1.66
	RMSE	4.57	3.69	4.11	9.63	7.09	8.36	1.51	1.80	1.71

[c]Note RMSE is the root mean square error, r is the linear correlation coefficient, Error STD is the error standard deviation, RMSE is root mean square error

under predicted. For temperature and wind speed, the bias is significantly less than the error standard deviation (Error STD). This suggests that the random error component of the model is contributing more significantly to the simulations overall error than systematic errors.

Upper level atmospheric patterns were compared at 00Z (1600 PST) for each day. Figure 3.5 shows the comparison on three different days which represent the general vertical profiles seen in MM5 predicted temperatures, mixing ratio, wind speed and wind direction. On most days the vertical temperature and wind speed profiles agree with observed profiles in both the vertical structure and in magnitude. Mixing ratio and wind speed both show that although the model does seem to produce the general vertical structure as the observations, it does not do nearly as good of a job of capturing correct magnitudes as it did with temperature. MM5 estimates a moisture bias within the lower 3 km of the atmosphere. Comparisons between MM5 vertical estimations and observations on August 31 show more disagreement than is seen on previous days. Simulated vertical temperatures are slightly warmer than the observations and wind speeds are overestimated by about 2-3 m s^{-1}. The disagreements between observations and simulations seen on August 31 were unusual and are most likely due to the northerly direction of near surface and upper level winds. As these moves in from the complex terrain of the north it is harder for the model to simulate the meteorological conditions compared to previous days when the surface winds were coming from the west, over the smooth surface of the ocean. Simulated wind directions on all three days agree well with observations. While there are some clear disagreements between the predicted and the observed meteorological fields both at the surface and aloft, the overall performance of

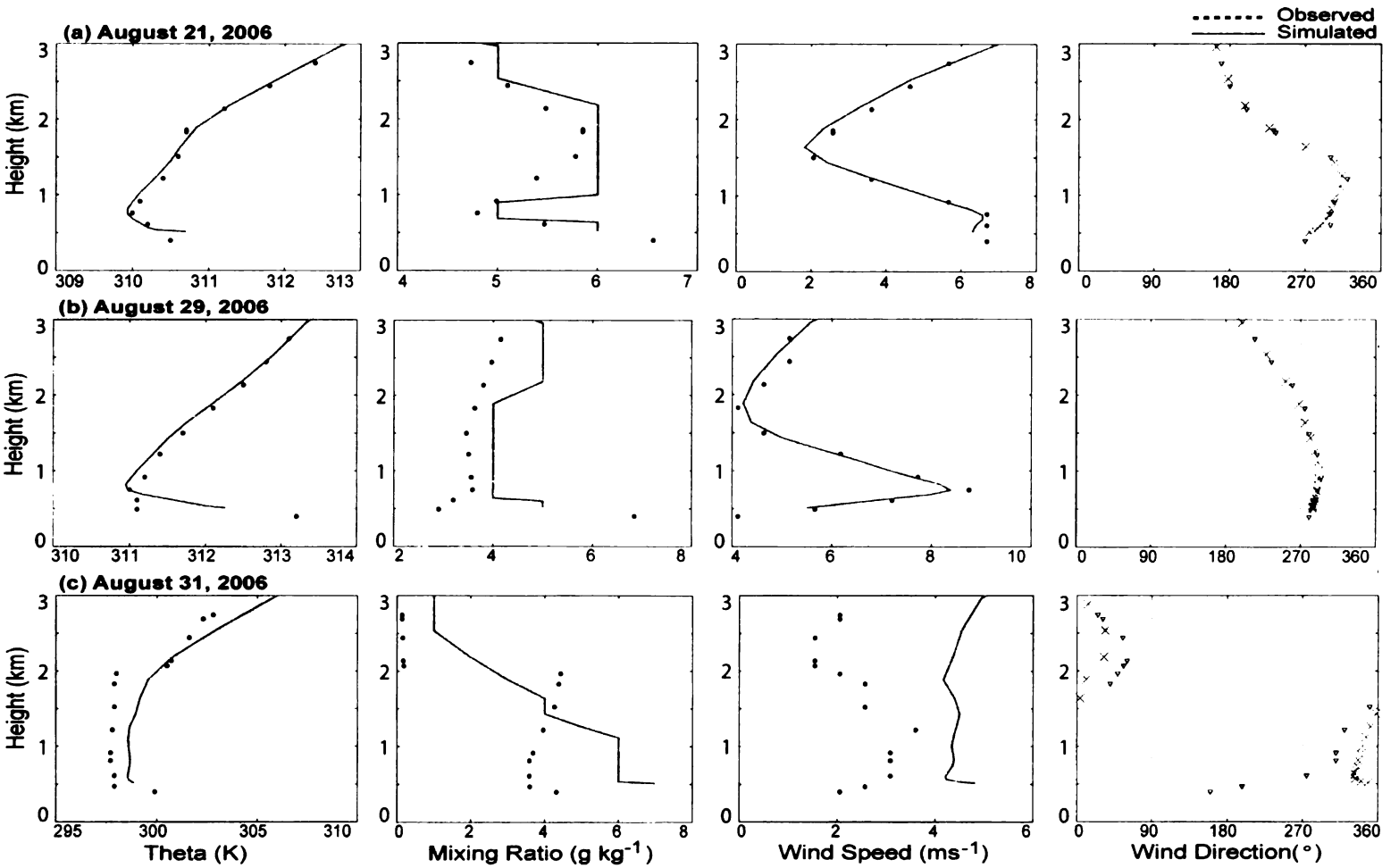

Figure 3.5 Upper level patterns at 00Z (1600 PST) Medford, Oregon station at three different dates (a) August 21, 2006, (b) August 29, 2006, and (c) August 31, 2006. Variables examined are theta, mixing ratio, wind speed and wind direction; all plotted against height. Black dotted lines and upside down triangles (wind direction) represent observations while gray lines and x's (wind direction) represent MM5 simulated meteorological conditions.

the model in this region is good especially considering the highly complex topography and land cover.

Smoke Plume and $PM_{2.5}$ Prediction

Aerosol optical depth (AOD) data and BlueSky estimations (Figure 3.6) indicate high correlation in aerosol concentration peaks and plume locations. Figure 3.6a shows a peak in AOD values off the coast of northern California which is represented in the BlueSky images as well. MODIS HMS imagery displays this plume as well, showing the located in similar south-northwest orientation – all of which are consistent with the synoptic conditions and the southerly winds on August 21. On August 29 (Figure 3.6b), BlueSky detects the smoke plume over northern California and its southwest-northeast orientation – which agrees with the HMS imagery. BlueSky also shows slightly higher aerosol concentrations over central-northern California, in comparison to central California, again in agreement with the AOD values shown. MODIS HMS does not show the higher aerosol concentrations over central Nevada, which is evident in both BlueSky and the AOD images. This is most likely due to the low intensity (thus low heat) of the fire or the existence of low, thick clouds during the observation times, which prevents the satellite from picking out the fire from its surroundings. The AOD image is able to pick up this increase because its not trying to distinguish the fire from the background, it is measuring the amount of light that is able to pass through the atmosphere. A similar situation is found in Figure 3.6c, where BlueSky, HMS, and AOD identify a plume off the coast of northern CA, but HMS does not pick up the smoke

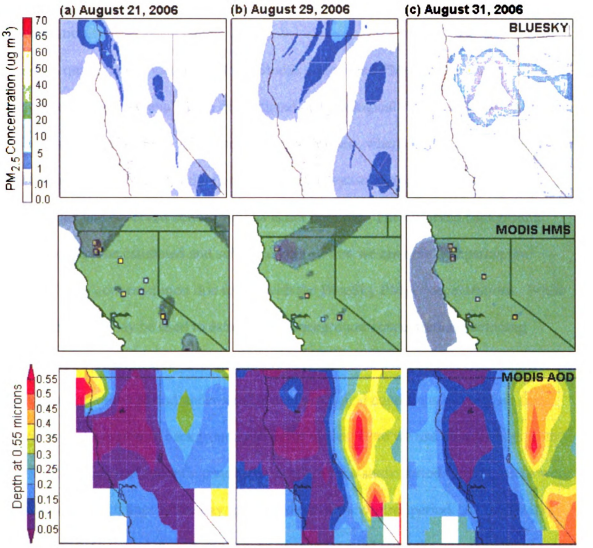

Figure 3.6. The images across the top show BlueSky visual output of surface $PM_{2.5}$ concentrations for three days (a) August 21, (b) August 29 and (c) August 31. The middle images show the corresponding satellite data taken from MODIS hazard mapping system (HMS), where gray shading indicates significant smoke plumes. Darker shades of gray represent higher concentrations of smoke. The bottom images are the aerosol optical depth data for each day, also taken from MODIS. Warmer colors indicate a higher concentration of aerosol within the atmosphere.

plume evident in Nevada. In most instances, BlueSky is able to simulate the existence, orientation and shape of observed smoke plumes and areas of higher aerosol concentration.

A quantitative evaluation of the BlueSky-predicted $PM_{2.5}$ concentration is not as straight forward as the evaluation of predicted meteorological fields. $PM_{2.5}$ observations include both a background value and a fire contribution, whereas BlueSky predicted PM concentrations only consider the fire emissions. Because of this, a direct comparison of the modeled and observed concentrations is not possible. The observed background value must first be estimated and subtracted out so that we are only comparing the observed $PM_{2.5}$ concentration due to fire with the BlueSky $PM_{2.5}$ concentrations. While several methods may be used to estimate the background concentration, including running a photochemical model, one simple approach is to use PM observations from the same sites for a time period under similar meteorological conditions but with no fire activities in the region as background reference values. Here we use observations from July 16-24 which had synoptic conditions similar to the study period. Mean values were calculated for each hour of the day for the 9 days of the control period. At each station during the study period these mean values were subtracted from the observed hourly values. The subtraction may yield a negative value in some cases, which means that the observed $PM_{2.5}$ value at that particular hour is lower than average values for similar conditions. The observed values are non-zero and vary with time. This is because that the observed $PM_{2.5}$ concentrations are from both primary and secondary sources and some of these sources may differ from the period used for the calculation of the 'background values'. In addition, the meteorological conditions during the simulations period were

not exactly the same as the period used for background calculation. Although this is a relatively crude way to take into account the background PM concentration, the comparison between observed and estimated surface $PM_{2.5}$ concentrations should reveal how well the BlueSky predictions estimate the increase of PM concentration due to the fires at a particular location.

Comparisons of BlueSky-predicted hourly $PM_{2.5}$ concentrations with the adjusted observations are shown in Figure 3.7 for the eight monitoring sites within the domain. Since BlueSky only considers $PM_{2.5}$ emissions from fires, the predicted $PM_{2.5}$ concentrations at each site is zero except for times when a smoke plume from the fires were advected to the location. Despite these complications, the comparisons show that the BlueSky predicted $PM_{2.5}$ concentrations appear to emulate the observed peaks although the timing of the peaks may not be the same in some instances. The magnitudes of large increases in $PM_{2.5}$ are comparable to observations, an important distinction not seen in previous studies (Adkins et al. 2003; Berg et al. 2003; Larkin et al. 2007). At all stations, it appears that BlueSky does a better job capturing predicted surface concentrations of $PM_{2.5}$, in terms of both magnitude and timing, when the observed concentrations are higher than 10 $\mu g\ m^{-3}$. The passage of the smoke plume that was traveling to the northeast on August 29 (Figure 3.6b) is visible in the surface concentrations of the stations located in the northern section of the study area (Figures 3.7a, 3.7b, 3.7c, and 3.7d) as an increase in $PM_{2.5}$ concentrations is evident in both the model results and the observations. At all four of these stations the simulated $PM_{2.5}$ increase occurred approximately 24 hours before the increase is seen in the observations. This is most likely due to the overestimated model wind speeds during previous days

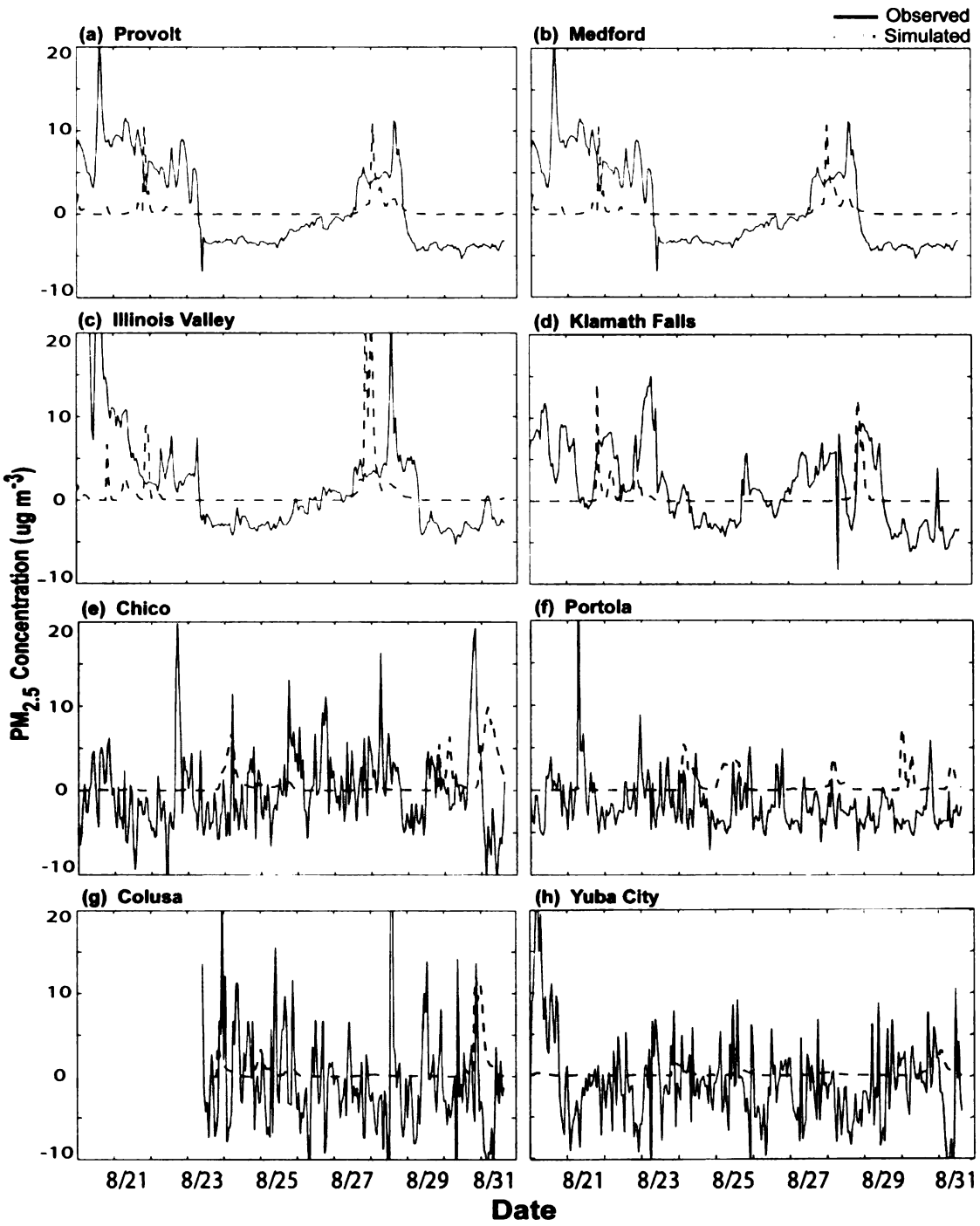

Figure 3.7. Hourly $PM_{2.5}$ concentrations at the 8 monitoring stations located in northern California and southern Oregon. Solid black lines represent the observed adjusted concentrations of $PM_{2.5}$ while the gray dotted lines indicate the BlueSky estimated $PM_{2.5}$ concentrations.

(Figure 3.4b and 3.4c), causing the smoke to be advected into these regions prematurely. BlueSky was not able to predict the large increases seen in the observed concentration in Figures 3.7e, 3.7f and 3.7h near the beginning and the middle of the study period. All of these stations (except for Portola, Figure 3.7f) are found at elevations lower than 100 m and are located in the northern section of the Central Valley. A disadvantage of using single station time series in comparing $PM_{2.5}$ concentrations is the dependence of each station to the location of the simulated smoke plume. For instance, a simulated smoke plume may miss a station's location by only one model grid point and the expected increase in $PM_{2.5}$ is then not produced by the simulation, giving an impression that the BlueSky simulations to severely under-predict surface $PM_{2.5}$ concentrations. While this may be true, the under-prediction may also just be due to the "miss" of the smoke plume due to differences in the simulated and observed upper level meteorological patterns in wind speed and direction. Other possible explanations in BlueSky concentration errors are uncertainties within the BlueSky framework itself. According to Larkin *et al* (2007), fuel loadings (which are largely unknown for the majority of fires) and the consumption calculations (which are dependent upon the fuel loadings) are two large sources of uncertainty. The above results indicate that while some large increases of surface $PM_{2.5}$ concentrations are accurately estimated by BlueSky, there is a need to improve these predictions so that all of the observed increases in $PM_{2.5}$ are estimated, regardless of their magnitude.

Summary and Conclusion

BlueSky is a smoke modeling framework that integrates consumption, emissions, meteorology, and dispersion models to predict surface concentrations of air pollutants, such as $PM_{2.5}$. BlueSky also provides the users with visual images of projected smoke plume trajectories and shape. This framework is being used by smoke managers and burn bosses to make 'go' and 'no-go' decisions concerning prescribed burns. Lately, BlueSky is also being used in management decisions concerning wildfires and wildland fire use fires. Despite its popularity, limited validation has been performed and the uncertainties of the model under conditions different than those common in the Pacific Northwest are largely unknown. The purpose of this study is to compare BlueSky predicted surface $PM_{2.5}$ concentrations with in-situ observations and to compare smoke plume shape and trajectories with remotely sensed images of significant smoke plumes and aerosol optical depth to qualitatively assess the accuracy of BlueSky predicted results.

The performance of the MM5 model in estimating meteorological fields were evaluated first as accurate meteorological conditions are essential to the transport and dispersion of PM from fires. The simulations captured the trend and day-to-day variation in temperature and wind speeds due to changes in synoptic conditions. In most cases, the simulated temperatures were found to have a large warm bias during the nighttime and a cold bias during the day, leading to an overall smaller diurnal range than is actually observed. The simulations tended to overestimate wind speed for near calm conditions while the underpredicted wind speeds for strong wind conditions. On most days, the simulated wind directions, however, agree quite well with the observations. The

simulated vertical profiles of wind speed, direction, potential temperature, and mixing ratio are also in good agreement with the rawinsonde observations with the exception of August 31 which was under different synoptic conditions than the rest of the study period. On all days, there is a wet bias in the lower atmosphere up to 3 km, and a cold bias in the lower atmosphere. The model reproduced the observed wind direction and vertical shear of the wind direction, which is very important for transport simulations.

Next, $PM_{2.5}$ surface concentrations and trajectories simulated from BlueSky were compared with observations. It is difficult to quantitatively compare BlueSky predicted $PM_{2.5}$ concentrations with observations as the latter contain PM concentrations from all sources, not just from fire emissions. At each station, a 'background value' was estimated for each hour of the day using hourly averages from a fire-free period with similar weather conditions. The comparison of the simulated and observed hourly $PM_{2.5}$ concentrations at eight stations indicate that BlueSky is in general able to simulate the observed large increases in $PM_{2.5}$, although there are some discrepancies in the simulated and observed timing of the peaks in some cases. Comparisons of the BlueSky predicted particle plumes with the satellite images show reasonable agreement in the orientation and aerial extension of the fire plumes.

This study shows that the BlueSky smoke modeling system can serve as a tool for estimating long range transport of smoke plumes. BlueSky can be used to assess smoke plume shape and orientation, but it needs improvement in capturing the magnitudes of increases in $PM_{2.5}$ concentrations. More accurate reporting of wildfire size and locations within the national ICS-209 reports, provided by fire managers, will help to improve emissions estimations within BlueSky. Also, sensitivity studies of the emissions and

consumption models are useful to help identify areas of uncertainty within these models. Removing these uncertainties and improving each models estimations will lead to increased accuracy of the BlueSky predicted surface concentrations as well as the overall model performance.

PART IV

SOUTHERN CALIFORNIA, OCTOBER 2007

Introduction

On October 20, 2007, a series of wildfires broke out across southern California. For the following 19 days, aided by unusually strong Santa Ana Winds (gusting as high as 140 km/hr) and hot, dry conditions, these wildfires destroyed 1500 homes, burned over 500,000 forested acres, caused 9 deaths and 85 injuries, and forced over 900,000 people to be evacuated (the largest evacuation in the history of California) (Flaccus 2007). A state of emergency was declared in seven counties (Archibold 2007) and extensive power outages occurred throughout the region. At the height of the extreme, wind-driven fire activity, 17 separate fires were burning and PM_{10} and $PM_{2.5}$ concentrations reached and maintained unhealthy levels for several hours. The extensive destruction and publicity caused local, state and federal agencies to closely examine the protocols used in the suppression efforts to aid in prevention and suppression of future outbreaks.

In addition to direct fire threats of loss of life, property and wildlife, secondary threats such as reduced visibility and increased air pollution also exist, making it unsafe to be outdoors. Air quality and wildfire managers need to be able to make fast and accurate decisions about impending risks current fires and their accompanying smoke release may cause, and they must be able to convey that information to the public. The EPA has been instrumental in establishing air quality initiatives, setting air pollution standards and aiding in the design and implementation of numerous air quality models (Agency 2006).

Modeling of aerosol dispersion over the western United States is complicated by the mountainous terrain which greatly affects this region's meteorology (Kim and Stockwell 2007). Furthermore, the long-term effects of smoke are dependent upon the fire environment and the fires characteristics (Reinhardt, Keane, and Brown 2001), further increasing the complexity of modeling smoke dispersion in the West. Several models, such as CALPUFF (Scire, Strimaitis, and Yamartino 2000), SASEM (Sestak and Riebau 1988), VSMOKE (Lavdas 1996), and TSARS Plus (Hummel and Rafsnider 1995) have been designed to predict fire emissions, but these models are either too simplistic to represent the complexity of smoke dispersion in complex terrain, or too complex to be implemented by users with limited computer experience and/or scientific background. In order to simulate smoke dispersion and the subsequent effects on air quality, dispersion models must integrate fire spread, fire emissions, atmospheric flow, smoke dispersion and chemical reactions (Miranda 2004). Clearly, a balance must be maintained between the components needed to accurately simulate smoke dispersion and a user-friendly interface that allows the model to be utilized for different applications.

In early 2000, under the National Fire Plan, the USDA Forest Service AirFire team launched a modeling system that predicts smoke trajectories and ground concentrations from wildland fires (Ferguson, Peterson, and Acheson 2001). This framework, coined BlueSky, integrates meteorology, emissions, dispersion and trajectory models to produce these estimations and the results are made available to fire managers and air resource regulators. BlueSky is an interactive tool where users can choose which components they need, and when used along with GIS, users can zoom in on areas of interest, step through time, and overlay other GIS layers (geopolitical boundaries,

meteorological fields, topography, etc) in order to interactively view mapped information and analyze the underlying data (O'Neill et al. 2005).

BlueSky was designed with the users in mind, with necessary input requirements limited to only fire information such as date and location. After the information is entered BlueSky employs a mesoscale model, to provide feedback on wildland fire smoke impacts. Other secondary information can be provided, but if additional information is not available, default values are obtained from specified databases and look-up tables. Originally designed as a tool for making 'go' and 'no-go' decisions for prescribed burns, BlueSky's applications have been expanded to include smoke impact assessments concerning wildland fire use (WFU) fires and wildfires. Evaluation of the framework has been focused mainly on fires in the Pacific Northwest (Adkins et al. 2003; Berg et al. 2003; Larkin et al. 2007; BSRW 2006) and Southeast (Pouliot et al. 2005; Craig et al. 2007).

Although none of the existing validation efforts have been subjected to peer review, many of the studies listed above have produced similar results. In a study focused on the 2002 Hayman Fire in Colorado, Adkins *et al* (2003) found the location and timing of predicted smoke impacts to agree with observations while the predicted $PM_{2.5}$ concentrations were orders of magnitudes smaller than observations. Larkin *et al* (2007) conducted a similar study using data collected during the 2001 Rex Creek Wildfire in Washington and the 2005 Frank Church Wildfire in Idaho. Similar to Adkins *et al* (2003), the comparisons between smoke plume trajectories and shapes were found to agree quite well with satellite images, but BlueSky again failed to accurately predict the observed magnitudes of $PM_{2.5}$ concentrations. Results from these studies show that while

BlueSky can accurately predict smoke trajectories and the timing of smoke impacts, predictions of ground concentrations are poor. This paper presents results of the performance of the BlueSky modeling framework in simulating smoke dispersion and surface $PM_{2.5}$ impacts from the October 2007 southern California wildfire outbreaks by using two different meteorological initialization data sets. The use of two different sets of initialization data will help to identify the sensitivity accurate meteorological estimations are to the overall performance of BlueSky.

Methods

Study Area

California's large area (almost 10° longitude and more than 30° latitude) leads to vastly different climate and vegetation types between the northern and southern areas of the state. Like the mountainous basin and range provinces of the north, southern California has varying topographical features such as hills, mountains, plains and mesas. The Transverse Range, which occupies an area approximately 482 km wide beginning near Point Arguello (southern California's western most point) to the east at the Little San Bernardino mountains, is the only east – west trending mountain and valley system in California (Durrenberger 1968). The Transverse Ranges western portion is occupied by the Los Angeles basin, an area of relatively flat topography, broken up by gentle hills and mesas and divided by the Newport – Inglewood fault zone. The eastern extent of southern California is separated from the rest of the United States by the Sierra Nevada mountain range. The highest peak is Mt Whitney at an elevation of 4,421 m (14,505 ft). The Sierra Nevada range aids in the creation of strong, dry, downslope adiabatic winds

known as the Santa Ana's. These winds occur when a high pressure system is located over the Great Basin and a low forms over the coast, causing warm and dry (due to their interior origination) winds to move from the east to the west accelerating through mountain passes.

Western California is bordered by the Pacific Ocean, which creates drastically different climate and vegetation patterns in the western, coastal regions than in the eastern, inland regions. The moderating effects of the ocean produce large differences between inland and coastal temperature and precipitation. Generally, near the coasts lower annual temperatures are seen, with yearly maximums ~20°C while approximately 250 km inland temperatures are ~28°C (WRCC 2008). Yearly total precipitation near the coast averages approximately 33 cm, while only one third of that amount falls over the inland area, as average rainfall is closer to 11 cm. Precipitation occurs predominately during the winter season, beginning in late October or November and persisting through May or June (Durrenberger 1968).

Vegetation patterns shift from thicker, dense forests at higher elevations to sparse oak forests, shrubs and chaparral at lower elevations, valley bottoms and near the coast. Ponderosa pine forests, composed of ponderosa pine, white fir, sugar pine, douglas fir and incense cedar, are found between 1,524 m and 2,438 m (MSL) and are the most extensive forests found within southern California (Durrenberger 1959). Near the upper reaches of the ponderosa pine forests, white fir and sugar pine intermix with red fir as the ponderosa pine forests transition to the red fir forests. Red fir forests are scattered and sparse over the landscape. Generally, the lower elevations of southern California are dominated by oak woodland and chaparral. In the oak woodland zones, oak trees occur

erratically across grass covered hills and valleys. Foothill woodlands, one of two types of oakland woodlands, are a transition zone between valley bottom prairie grasses and the forested slopes above (Durrenberger 1959). Chaparral, one of the most characteristic vegetation types of southern California, is composed of many different types of shrubs, but is dominated by evergreen plants. These shrubs have a long root system that allows them to survive the long, hot and dry summers of southern California. The ability to survive harsh conditions and a location on drier slopes makes chaparral an ideal fuel source for wildfires.

Model Setup and Simulation

There are two main components necessary for running the BlueSky Smoke Modeling framework: meteorology and fire input information. Predictions of the meteorological fields during October of 2007 were generated using the Pennsylvania State University/NCAR mesoscale model (MM5) (Grell, Dudhia, and Stauffer 1994). Terrain and domain information was provided by California and Nevada Smoke and Air Committee (CANSAC). Three nested domains were used, with the innermost 4 km domain covering the California and Nevada region, while the outermost 36 km domain encompassed the western US and eastern edge of the Pacific Ocean (Figure 4.1). To evaluate how BlueSky performs under different meteorological simulations, two different meteorological inputs were used. Initial and boundary conditions for the first simulation were provided by National Center for Environmental Prediction (NCEP) 40 km Eta forecasts and for the second simulation, initial and boundary conditions came from the NCEP 32 km North American Regional Reanalysis (NARR) output. BlueSky aerosol

transport and dispersion is simulated using CALPUFF, a 2 dimensional, non-steady state Lagrangian puff dispersion model which simulates time and space varying pollutant transport, transformation and removal (Scire, Strimaitis, and Yamartino 2000). The Satellite Mapping Automatic Reanalysis Tool for Fire Incident Reconciliation (SMARTFIRE) was used to obtain information on fire location, size and emissions. In order to create a comprehensive and spatially accurate data set, SMARTFIRE combines both wildfire incident data from the national wildfire (ICS-209) reports along with satellite-detected fire data (Craig et al. 2007). $PM_{2.5}$ emissions were calculated within BlueSky using Consume/EPM v1.03 while the Fuel Characteristic Classification System (FCCS) was used to obtain fuel characteristics information.

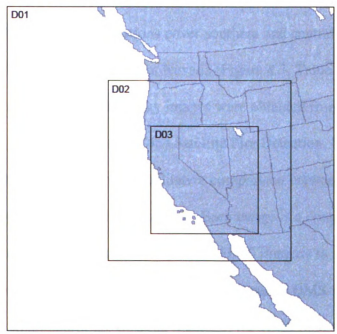

Figure 4.1. Modeling domains used within this study. D01 is the 36km domain, D02 is the 12km domain and D03 is the 4km domain. The 12km and 4km domains are one-way nested domains.

Surface and Satellite Observations

Surface meteorological parameters simulated by the PSU/NCAR Mesoscale Model (MM5) were validated against hourly surface data from the National Climatic Data Center website for 75 stations (Figure 4.2, Table 4.1) within the region. NCDC combines surface meteorological data from the National Weather Service (NWS) first-order, ASOS and COOP networks. Upper air observational data were obtained for six stations at 00Z (16 PST) and 12Z (0400 PST) from the University of Wyoming Weather Web website. The names of the upper air stations are listed on Figure 4.2. The output from the BlueSky Smoke Modeling Framework simulations includes hourly $PM_{2.5}$ concentrations and a visual image of the smoke plume shape and trajectory. To compare simulated surface concentrations of $PM_{2.5}$ to observed concentrations, hourly $PM_{2.5}$ observations were obtained from the AIRNow database and the California Air Resources Board (ARB) database. Sixty-one stations cover southern and central California, and five stations are located in nearby southeastern Nevada (Figure 4.3, Table 4.2). Satellite observations for comparison with BlueSky images were obtained from the Moderate Resolution Imaging Spectrometer (MODIS) Satellite Fire Detection, Hazard Mapping System (HMS). These images allow a qualitative comparison between simulated and observed smoke plume shapes and orientations. Each image is a composite of all detected smoke plumes for a given 24 hour period. HMS imagery is at times not in agreement with aerosol optical depth data due to limitations in HMS fire detection. When fires are too small and/or are of weak intensity, the HMS imagery has a difficult time in distinguishing the fire from the background, especially in the western United States summer season when surface temperatures are very hot. Also, satellites (using the

3.9 micron band) are not able to see through clouds other than cirrus, so fires occurring in those areas will go undetected (McNamara et al. 2004). To gain a more quantitative comparison with the concentrations of PM2.5 within the BlueSky predicted smoke plume, GOES Aerosol/Smoke Product (GASP) images are employed. These images are hourly displays of the concentration of aerosol in the atmosphere. GASP images represent the thickness of air columns due to aerosols (or other airborne particles). Higher AOD values indicate more aerosols in the column and so less light is able to pass through.

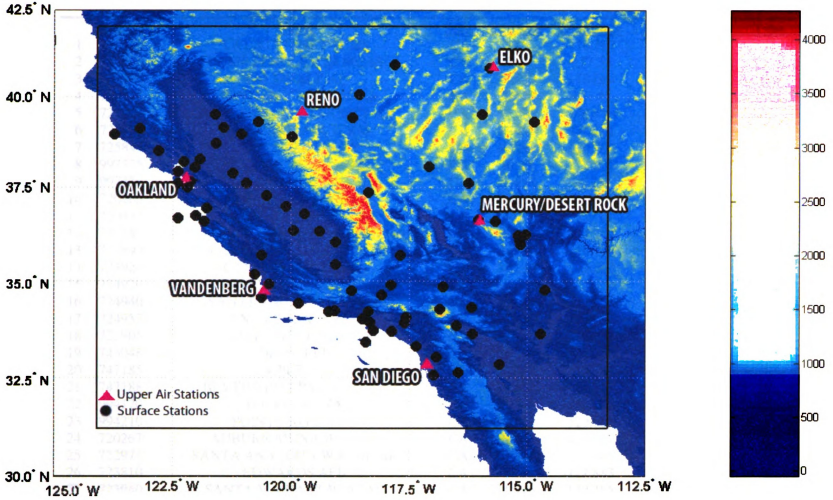

Figure 4.2 Hourly data from 75 surface meteorological stations and twice daily soundings from the 6 upper air stations were used to validate MM5 predictions during October 15 – 30, 2007. The black box indicates the 4km one-way nested domain used for the simulations. Black circles indicate surface stations while red triangles indicate an upper air station.

Table 4.1. Meteorological observation station geographic information[d]

	Site ID	Name	State	Latitude	Longitude	Elevation (m)	Type
1	690150	TWENTYNINE PALMS	CA	34.3	-116.167	695.9	S
2	722926	CAMP PENDLETON MCAS	CA	33.3	-117.35	23.8	S
3	723820	PALMDALE AP	CA	34.629	-118.084	787	S
4	724915	MONTEREY PENINSULA	CA	36.583	-121.85	50	S
5	724926	MODESTO CITY-COUNTY AP	CA	37.626	-120.953	29.6	S
6	724935	HAYWARD AIR TERM	CA	37.659	-122.121	14.3	S
7	725845	BLUE CANYON AP	CA	39.292	-120.708	1610.3	S
8	997375	MOORED BUOY 46092	CA	36.75	-122.017	4	S
9	997376	MOORED BUOY 46093	CA	36.683	-122.4	4	S
10	720165	BIG BEAR CITY AP	CA	34.267	-116.85	2057	S
11	720333	CORONA MUNICIPAL AP	CA	33.9	-117.6	163	S
12	722880	BURBANK-GLENDALE-PASSADENA AP	CA	34.201	-118.359	223.1	S
13	723890	FRESNO YOSEMITE INTL AP	CA	36.78	-119.719	99.7	S
14	723926	CAMARILLO (AWOS)	CA	34.217	-119.083	23	S
15	724920	STOCKTON METR AP	CA	37.894	-121.237	8.2	S
16	724940	SAN FRANCISCO INTL AP	CA	37.62	-122.398	5.5	S
17	724957	SANTA ROSA (AWOS)	CA	38.509	-122.812	45.1	S
18	725905	UKIAH MUNICIPAL AP	CA	39.126	-123.201	190.8	S
19	745048	OROVILLE	CA	39.5	-121.617	57	S
20	747185	IMPERIAL	CA	32.833	-115.583	17	S
21	747188	BLYTHE RIVERSIDE CO AP	CA	33.619	-114.717	119.5	S
22	994120	POINT ARENA	CA	38.95	-123.733	19	S
23	994210	POINT ARGUELLO	CA	34.567	-120.633	34	S
24	720267	AUBURN MUNICIPAL AP	CA	38.95	-121.067	467	S
25	722977	SANTA ANA JOHN WAYNE AP	CA	33.68	-117.866	16.8	S
26	723810	EDWARDS AFB	CA	34.9	-117.883	705.9	S
27	723940	SANTA MARIA PUBLIC AP	CA	34.916	-120.465	72.5	S

[d]'S' signifies surface meteorological observations while 'U' signifies upper air observations

Table 4.1. Continued[d]

	Site ID	Name	State	Latitude	Longitude	Elevation (m)	Type
28	724815	MERCED/MACREADY FLD	CA	37.283	-120.517	47	S
29	725847	SOUTH LAKE TAHOE	CA	38.894	-119.995	1912	S
30	745160	TRAVIS AFB/FAIRFLD	CA	38.267	-121.933	18	S
31	746120	CHINA LAKE NAF	CA	35.683	-117.683	695.9	S
32	747040	ONTARIO INTL AP	CA	34.05	-117.567	287	S
33	747186	CAMPO (AWRS)	CA	32.616	-116.467	802	S
34	994023	PORT SAN LUIS	CA	35.183	-120.767	2	S
35	994028	SANTA MONICA	CA	34	-118.5	2	S
36	994035	LOS ANGELES	CA	33.717	-118.267	2	S
37	994036	RICHMOND	CA	37.933	-122.4	2	S
38	722904	SAN DIEGO/BROWN FLD	CA	32.567	-116.983	159.4	S
39	723830	SANDBERG	CA	34.744	-118.724	1378.6	S
40	723840	BAKERSFIELD MEADOWS FIELD	CA	35.434	-119.056	150	S
41	723896	VISALIA MUNI (AWOS)	CA	36.317	-119.4	89	S
42	724800	BISHOP AP	CA	37.373	-118.363	1263.4	S
43	724837	BEALE AFB/MARYSVILE	CA	39.133	-121.433	38.1	S
44	724839	SACRAMENTO METRO AP	CA	38.696	-121.59	10.1	S
45	745046	MADERA	CA	36.983	-120.117	77	S
46	745058	WATSONVILLE	CA	36.933	-121.783	48	S
47	994041	REDWOOD CITY	CA	37.5	-122.2	6	S
48	745056	RAMONA	CA	33.033	-116.917	424	S
49	994034	PORT CHICAGO	CA	38.05	-122.033	2	S
50	722868	PALM SPRINGS INTL AP	CA	33.833	-116.5	145	S
51	722920	SANTA CATALINA CATALINA AP	CA	33.405	-118.416	488.3	S
52	722956	JACK NORTHROP FLD H	CA	33.917	-118.333	21	S
53	723805	NEEDLES AP	CA	34.766	-114.623	278.6	S
54	723815	DAGGETT BARSTOW-DAGGETT AP	CA	34.854	-116.787	588	S
55	723895	PORTERVILLE (AWOS)	CA	36.033	-119.067	135	S

[d]'S' signifies surface meteorological observations while 'U' signifies upper air observations

Table 4.1. Continued[d]

	Site ID	Name	State	Latitude	Longitude	Elevation (m)	Type
56	723925	SANTA BARBARA MUNICIPAL AP	CA	34.426	-119.844	6.1	S
57	723927	OXNARD AP	CA	34.201	-119.206	20.7	S
58	723965	PASO ROBLES MUNICIPAL AP	CA	35.673	-120.627	249	S
59	724955	NAPA CO. AP	CA	38.213	-122.28	17.1	S
60	747020	LEMOORE REEVES NAS	CA	36.333	-119.95	71.3	S
61	747187	PALM SPRINGS THERMAL AP	CA	33.628	-116.16	36	S
62	722096	HENDERSON EXECUTIVE	NV	35.967	-115.133	749	S
63	722825	TONOPAH RANGE #74	NV	37.617	-116.25	1756	S
64	723860	LAS VEGAS MCCARRAN INTL AP	NV	36.079	-115.155	664.5	S
65	723865	NELLIS AFB	NV	36.233	-115.033	573	S
66	723870	MERCURY DESERT ROCK AP	NV	36.621	-116.028	1008.9	S
67	724846	N LAS VEGAS	NV	36.217	-115.2	671	S
68	724855	TONOPAH AIRPORT	NV	38.06	-117.087	1656.3	S
69	724860	ELY YELLAND FIELD	NV	39.295	-114.845	1908.7	S
70	724885	FALLON NAAS	NV	39.417	-118.7	1199.1	S
71	725805	LOVELOCK DERBY FIELD	NV	40.066	-118.565	1189.9	S
72	725824	EUREKA (RAMOS)	NV	39.517	-115.967	1993	S
73	725825	ELKO MUNICIPAL AP	NV	40.825	-115.792	1546.6	S
74	725830	WINNEMUCCA MUNICIPAL AP	NV	40.902	-117.807	1314.9	S
75	746141	CREECH AFB	NV	36.583	-115.667	955	S
76	72493	OAKLAND INT	CA	37.75	-122.22	1.82	U
77	72393	VANDENBERG AFB	CA	34.75	-120.57	36.88	U
78	72293	SAN DIEGO/MIRAMAR	CA	32.83	-117.12	40.84	U
79	72387	MERCURY/DESERT ROCK	NV	36.62	-116.02	306.63	U
80	72489	RENO	NV	39.57	-119.78	462.07	U
81	72582	ELKO	NV	40.85	-115.73	485.55	U

[d]'S' signifies surface meteorological observations while 'U' signifies upper air observations

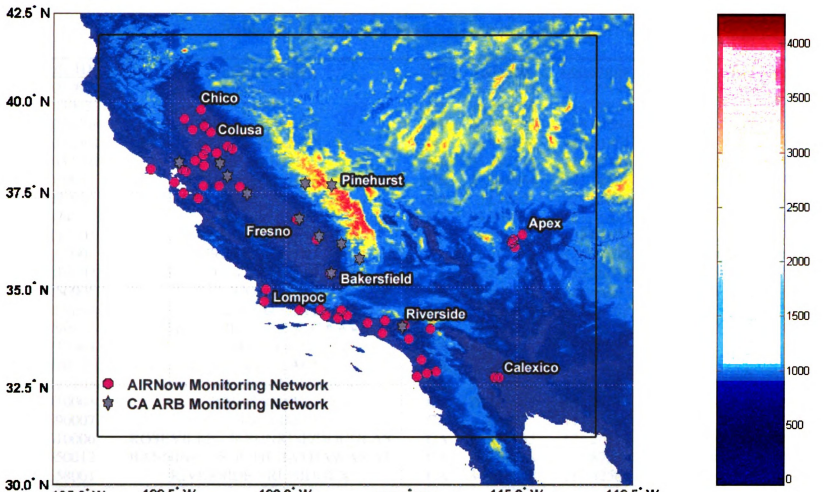

Figure 4.3 Surface particulate matter ($PM_{2.5}$) monitoring stations where hourly $PM_{2.5}$ data was obtained from the AIRNow monitoring sensors (circles) and the California Air Resources Board (ARB) monitoring sensors (stars). The black box indicates the 4km one-way nested domain used for the simulations.

Table 4.2. $PM_{2.5}$ observation station geographic information

	Site ID	Name of Station	State	Latitude	Longitude	Elevation (m)	Network
1	320030020	CRAIG RD	NV	36.245278	-115.09194		AIRNow
2	320030022	APEX	NV	36.390556	-114.90639	776	AIRNow
3	320030298	GREEN VALLEY	NV	36.052222	-115.05694	884	AIRNow
4	320030561	SUNRISE ACRES	NV	36.163056	-115.11361		AIRNow
5	320032002	J.D. SMITH	NV	36.191111	-115.12194		AIRNow
6	60010007	LIVERMORE - RINCON	CA	37.686944	-121.78306	145	AIRNow
7	60070002	CHICO - MANZANITA	CA	39.7575	-121.84222	62	AIRNow
8	60074001	GRIDLEY	CA	39.308333	-121.75833	29	AIRNow
9	60111002	COLUSA - SUNRISE BLVD	CA	39.203056	-122.01694	17	AIRNow
10	60190008	FRESNO – 1ST ST	CA	36.781389	-119.77222	98	AIRNow
11	60210002	WILLOWS – E LAUREL ST	CA	39.5175	-122.19028	41	AIRNow
12	60250005	CALEXICO – ETHEL ST	CA	32.676111	-115.48333	1.8	AIRNow
13	60250006	CALEXICO - EAST	CA	32.677778	-115.38972	10	AIRNow
14	60290014	BAKERSFIELD - 5558 CA AVE	CA	35.356111	-119.04028	117	AIRNow
15	60310004	CORCORAN	CA	36.25	-119.33333	62	AIRNow
16	60370016	GLENDORA - LAUREL	CA	34.143889	-117.85083	84	AIRNow
17	60371103	LOS ANGELES - N. MAIN ST	CA	34.066944	-118.24167	87	AIRNow
18	60410003	POINT REYES	CA	38.126944	-122.91389	24	AIRNow
19	60590007	ANAHEIM	CA	33.82	-117.91306	61	AIRNow
20	60610006	ROSEVILLE - N.SUNRISE/DOUGLAS	CA	38.745833	-121.26528	49	AIRNow
21	60650012	BANNING – SOUTH HATHAWAY ST	CA	33.927778	-116.87333	144	AIRNow
22	60658001	RIVERSIDE - RUBIDOUX	CA	34.010278	-117.42583	250	AIRNow

Table 4.2. Continued

	Site ID	Name of Station	State	Latitude	Longitude	Elevation (m)	Network
23	60659001	LAKE ELSINORE - W. FLINT ST	CA	33.674722	-117.33583	402	AIRNow
24	60670010	SACRAMENTO - T ST	CA	38.558333	-121.49194	5	AIRNow
25	60670012	FOLSOM	CA	38.683889	-121.16278	84	AIRNow
26	60730003	EL CAJON – REDWOOD AVE	CA	32.791389	-116.94167	132	AIRNow
27	60731002	ESCONDIDO	CA	33.127778	-117.07417	192	AIRNow
28	60731006	ALPINE	CA	32.833333	-116.75	375	AIRNow
29	60731010	SAN DIEGO - BEARDSLEY ST	CA	32.715278	-117.15417	56	AIRNow
30	60750005	SAN FRANCISCO – ARKANSAS ST	CA	37.765833	-122.39778	1	AIRNow
31	60773005	TRACY AIRPORT	CA	37.6825	-121.44056	60	AIRNow
32	60811001	REDWOOD CITY	CA	37.482778	-122.20222	5	AIRNow
33	60830011	SANTA BARBARA	CA	34.4275	-119.69028	110	AIRNow
34	60831008	SANTA MARIA - BROADWAY	CA	34.948056	-120.43444	76	AIRNow
35	60832004	LOMPOC H ST	CA	34.637778	-120.45667	26	AIRNow
36	60850005	SAN JOSE - JASKSON ST	CA	37.348333	-121.89472	9	AIRNow
37	60953002	VACAVILLE	CA	38.3525	-121.96167	48	AIRNow
38	60959999	RIO VISTA	CA	38.218333	-121.77	11	AIRNow
39	60990005	MODESTO – 14TH ST	CA	37.658333	-120.99361	27	AIRNow
40	61010003	YUBA CITY	CA	39.138889	-121.6175	20	AIRNow
41	61110007	THOUSAND OAKS – MOORPARK RD	CA	34.21	-118.86944	71	AIRNow
42	61110009	PIRU- PACIFIC	CA	34.404444	-118.81		AIRNow
43	61111004	OJAI – OJAI AVE	CA	34.416667	-119.24583	80	AIRNow
44	61112002	SIMI VALLEY – COCHRAN ST	CA	34.2775	-118.68472	94	AIRNow
45	61113001	EL RIO – RIO MESA SCHOOL #2	CA	34.265278	-119.13361	10	AIRNow

Table 4.2. Continued

	Site ID	Name of Station	State	Latitude	Longitude	Elevation (m)	Network
46	61130004	DAVIS	CA	38.533333	-121.775	18	AIRNow
47	61131003	WOODLAND	CA	38.661944	-121.72778	21	AIRNow
48	60950004	VALLEJO - 304 TUOLUMNE ST	CA	38.102222	-122.23667	2	AIRNow
49	60950006	BENICIA	CA	38.065556	-122.15056	182	AIRNow
50	5274	PINEHURST – FOREST SERVICE	CA	37.6955	-119.02	1250	CA ARB
51	2353	YOSEMITE VILLAG –VISITOR CENTER	CA	37.7486	-119.59	372	CA ARB
52	2655	NAPA – JEFFERSON AVE	CA	38.3114	-122.3	7	CA ARB
53	3026	CLOVIS - N VILLA AVE	CA	36.8194	-119.72	26	CA ARB
54	2094	STOCKTON – HAZELTON ST	CA	37.9517	-121.27	6	CA ARB
55	2996	TURLOCK - S MINARET ST	CA	37.4882	-120.84	17	CA ARB
56	5275	SPRINGVILLE – FOREST SERVICE	CA	36.1344	-118.81	322	CA ARB
57	2032	VISALIA - N CHURCH ST	CA	36.3325	-119.29	30	CA ARB
58	2977	ELK GROVE – BRUCEVILLE RD	CA	38.3025	-121.42	2	CA ARB
59	5273	KERNVILLE – FOREST SERVICE	CA	35.7533	-118.42	845	CA ARB
60	4004	MIRA LOMA – VAN BUREN	CA	33.9951	-117.49	219	CA ARB
61	3145	BAKERSFIELD – GOLDEN ST HWY	CA	35.3853	-119.01	151	CA ARB

Results and discussion

Wildland Fire and Synoptic Conditions During the Study Period

During the ten days prior to the extreme fire outbreaks, fire activity in southern California was minimal with. Major changes occurred on October 22nd as nineteen new fires were reported, ten of which were large and uncontained. Firefighters in the southern California counties of Los Angeles, Ventura, Orange, Santa Barbara, Riverside, San Diego, and San Bernardino battled extreme, wind-driven fire behavior for the next five days. While the number of large fires did not increase again during this period, many smaller fires ignited, at times as many as forty a day. October 27th finally brought relief to the fire fighters as only moderate, minimal and smoldering fire activities were reported. By October 30th fire fighters were able to get five large fires contained and by November that number had increased to eight. The Poomacha and Santiago fires were the longest lasting fires, with full containment not achieved until November 9th.

At the beginning of the study period, when fire activity was minimal, the west cost was under the influence of a strong upper level ridge. Beginning on October 15, a strong trough off the southwest coast of Canada and an upper level ridge over Mexico caused moderate (12 -15 m s^{-1}) 500 hPa west-southwesterly winds over the U.S. west coast. As this trough over Canada continued to move east, the upper level ridge over Mexico moved north, and by October 18 a strong 500 hPa contour gradient was created between the two regions (Figure 4.4a). Wind flow during this time was generally zonal with strong (35 - 40 m s $^{-1}$) westerly 500 hPa winds over the western U.S. By the 21st the ridge had moved off to the east, and the west coast was dominated by a strong upper level trough, causing 500 hPa northwesterly winds over most of California and Nevada,

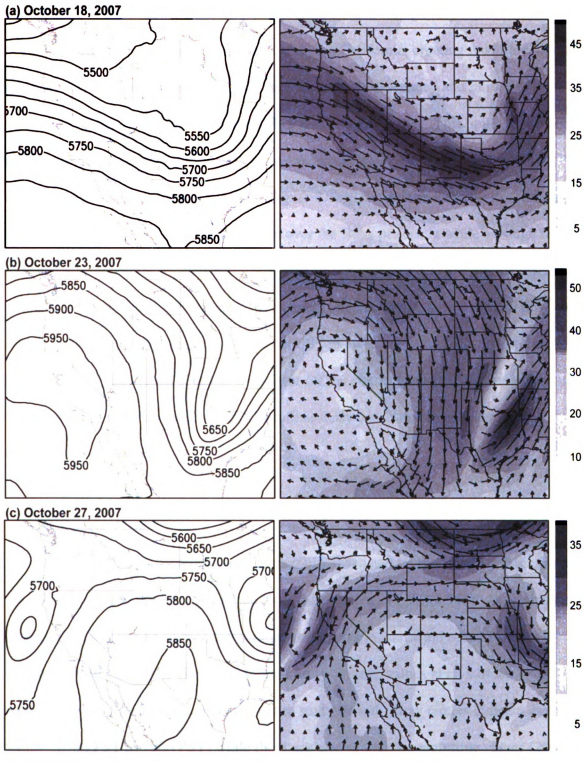

Figure 4.4 Plots of 500 hPa height (left) and wind speed (right) synoptic plots at 00Z (1600 PST). Light shading in the wind speed panels (right) indicates weaker 500 hPa wind speeds while darker shading indicates stronger wind speeds. Contours in the left panel represent 500 hPa isoheights.

contributing to the extreme wildfire activity. This system was quickly replaced with a upper level ridge, building off the coast of southern California, creating moderate, north-northeasterly 500 hPa winds over California. As this air descended and moved to the west of the Sierra Nevadas, they increased in intensity and speed. This upper level ridge dominated the west coast for the next three days, creating moderate (5-15 m s^{-1}) 500 hPa easterly winds over southern California (Figure 4.4b). During the morning of October 26th another upper level rige began to form over the Baha peninsula while a trough began to form over the Pacific Northwest. These two systems created 500 hPa southwesterly winds ranging in speed from 10 m s^{-1} near central and southern California to 25 m s^{-1} in northern California. By October 27th the cut-off low over the Pacific Northwest was developed and had moved south so it was just off the coast of central California (Figure 4.4c), and light to moderate (5-10 m s^{-1})southwesterly winds dominated southern California.

Meteorological Fields

The smoke and aerosol predictions simulated by the BlueSky framework are dependent upon the accuracy of the input information. Figure 4.5 is a comparison of simulated and observed surface temperature, mixing ratio, and wind speed for both the Eta and NARR runs. The circles represent hourly average values at all surface meteorological stations throughout the entire study period. Gray circles indicate daytime values (0700 PST to 1900 PST) while the black circles indicate nighttime values (2000 PST to 0600 PST).

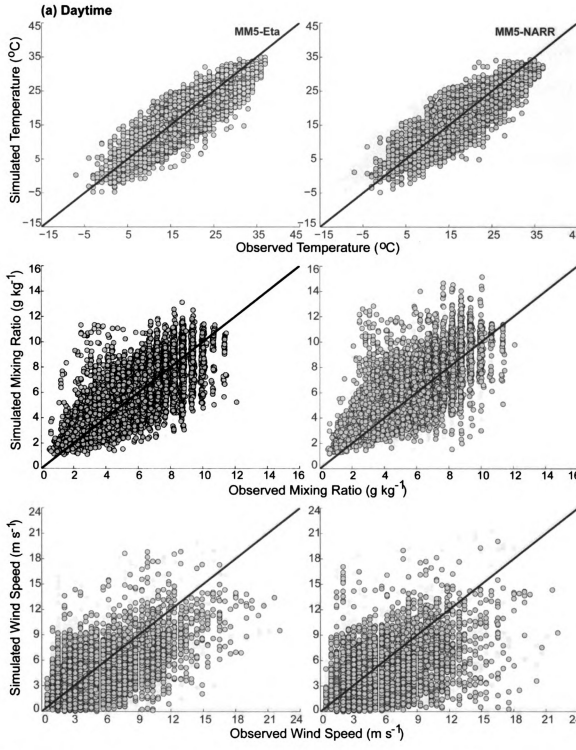

Figure 4.5 (a) Simulated and observed hourly temperature (top), mixing ratios (center), and wind speed (bottom) at all surface meteorological stations. Each circle indicates an hourly daytime average (0700 PST to 1900 PST).

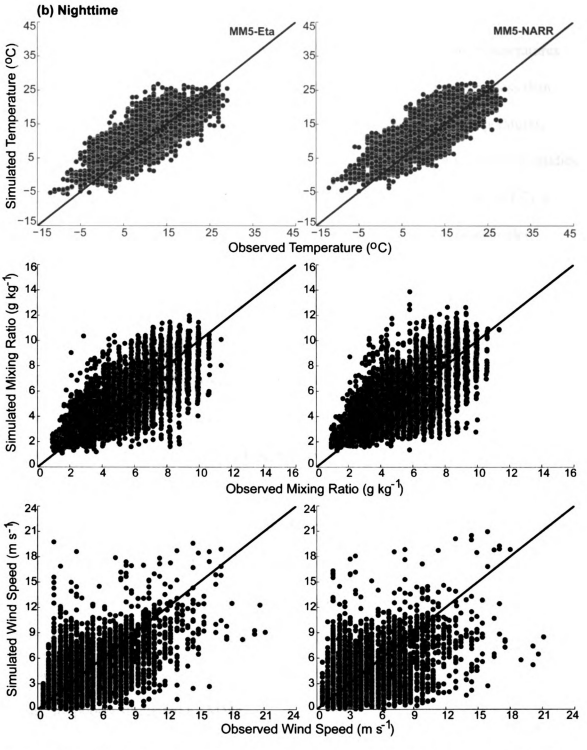

Figure 4.5 (b) Simulated and observed hourly temperature (top), mixing ratios (center), and wind speed (bottom) at all surface meteorological stations. Each circle indicates an hourly nighttime average (2000 PST to 0600 PST).

Simulated surface daytime temperatures in both models appear to have no distinct cold or warm bias when temperatures are below 25°C (77°F). As surface temperatures increase, a slight cold bias becomes apparent, with most discrepancies being less than five degrees. Comparisons between simulated and observed nighttime temperatures, however, show a warm bias in both simulations, which is consistent with previous studies (Zhong, In, and Clements 2007). Similar to what was found by Fusina *et al* (2007), a simulated nighttime warm bias along with a daytime cold bias, results in a smaller simulated diurnal temperature range. Consequently, the observed extreme (maximum and minimum) temperatures are not reached within the model.

The mixing ratio plots in Figure 4.5 show a small moisture bias evident within the model, especially when the mixing ratios are less than 5 g kg^{-1}. This is consistent with warmer nighttime temperatures and the resulting smaller diurnal cycle. The moist bias appears to be larger in the NARR simulations. As the mixing ratio values increase, the moist bias is not as pronounced as the plots show an increased scatter in both directions suggesting that the MM5 model has a difficult time estimating the increased amounts of moisture in the atmosphere. There also does not appear to be a difference between daytime and nighttime moisture biases, with both showing a large (moist) bias at the lower end (1-5 g kg^{-1}) of the mixing ratio scale. Daytime and nighttime wind speeds show an extremely large scatter which suggests that wind speeds, whether weak or strong, are poorly simulated by MM5.

Table 4.3 summarizes statistics (mean, RMSE, bias, correlation and error standard deviation) comparing the model with observations to help quantify the errors of the simulation. Simulated errors can be either systematic or random. Systematic errors

occur due to biases within the estimations and if known can be reduced through the use of calibration. Examples of systematic errors are misrepresentation of topography, land use properties and radiation. Random errors are due to uncertainty, whether it be in instrumentation and data collection or because of the grid spacing used within MM5. These types of errors can be reduced through statistical analysis. Examples of random errors are uncertainty within the observations themselves or the initial and boundary conditions used by a model.

Simulated standard deviations (STD), with the exception of NARR mixing ratios, are smaller than observed, indicating (as mentioned previously) that the model does not estimate the full extent of the temporal variations as seen in the observations. However, the model does do a better job at capturing the variations in wind speed and NARR mixing ratios as the STD between simulations and observations are comparable. Linear correlation coefficients (r) show strong correlations between simulated and observed temperatures and mixing ratios. NARR simulations indicate slightly higher temperature correlations ranging from 0.748 to 0.849 (Eta ranges from 0.747 to 0.861) while Eta simulations indicate slightly higher mixing ratio correlations, 0.810 to 0.825 (NARR from 0.775 to 0.805). Wind speed correlations also show moderately strong positive correlations, though slightly lower in both simulations than the other two variables. Wind speed coefficients range from 0.508 during NARR daytime to 0.668 during Eta nighttime. Bias is calculated by subtracting MM5 simulated temperatures, mixing ratios and wind speeds from observations. These values are then summed and then divided by the total number of observations to obtain an average. Day and nighttime temperature biases further illustrate what was seen in Figure 4.5, a slight warm bias at

Table 4.3. Meteorological comparison statistics for surface temperature, mixing ratio and wind speed[e]

		Temperature (°C)			Mixing Ratio (g kg^{-1})			Wind Speed (m s^{-1})		
	Statistics	Night	Day	All	Night	Day	All	Night	Day	All
Number of data points		11334	13336	24670	9454	11161	20615	11195	13263	24458
OBSERVATIONS	Mean	12.67	19.07	16.13	5.03	5.12	5.08	2.52	3.42	3.01
	STD	2.34	2.51	2.59	1.51	1.54	1.52	1.61	1.75	1.70
Eta	Mean	12.82	17.61	15.41	5.15	5.38	5.27	3.10	3.31	3.21
	STD	2.14	2.47	2.44	1.47	1.53	1.50	1.49	1.54	1.52
	Bias	0.15	-1.45	-0.71	0.12	0.25	0.19	0.57	-0.10	0.20
	r	0.747	0.883	0.861	0.810	0.825	0.818	0.569	0.668	0.627
	Error STD	3.67	3.01	3.43	1.38	1.40	1.39	2.28	2.30	2.32
	RMSE	3.67	3.34	3.50	1.38	1.42	1.40	2.35	2.31	2.32
NARR	Mean	13.41	17.98	15.89	5.32	5.71	5.53	3.29	3.48	3.40
	STD	2.12	2.51	2.39	1.51	1.58	1.55	1.53	1.57	1.56
	Bias	0.69	-1.11	-0.28	0.29	0.58	0.45	0.48	-0.20	0.11
	r	0.748	0.860	0.849	0.775	0.805	0.791	0.508	0.550	0.534
	Error STD	3.64	3.26	3.56	1.52	1.52	1.53	2.52	2.64	2.60
	RMSE	3.71	3.44	3.57	1.55	1.63	1.59	2.57	2.65	2.60

[e]Note RMSE is the root mean square error, r is the linear correlation coefficient, Error STD is the error standard deviation, RMSE is root mean square error

night, 0.15°C in the Eta simulation and 0.74°C in the NARR simulation. The Eta daytime cool bias is larger than NARR, -1.458°C compared to -1.195°C. Mixing ratio shows a weak bias, with the exception being the NARR daytime, which indicates a moist bias of 0.588 g kg^{-1}. A positive nighttime bias of ~0.5 m s^{-1} and negative daytime bias of 0.1 m s^{-1} is apparent in both simulations. For all variables in both simulations, the bias is less than the error standard deviation (Error STD). This suggests that the random error component of the model is contributing more to the simulations overall error than systematic errors.

Vertical profile comparisons of meteorological data at upper levels (up to 3 km) at the six different monitoring stations showed similar patterns. The vertical profiles shown in Figure 4.6 are from the San Diego, CA monitoring site, located at an elevation of less than 50 m. Compared to the other five stations, San Diego was the most impacted by the fires during the study period, especially during October 24-27, when the highest amount of fire activity occurred. Potential temperature comparisons at this station indicate that while both MM5 simulations are able to estimate the same profile shape as the observations, a warm bias of ~1-4°K exists that tends to increase with height. Mixing ratio comparisons for both simulations show that consistently, simulated mixing ratios are higher than observed. This moist bias continues with height in the Eta simulations while with the NARR simulations, the bias is largest at the lower levels and decreases with height. Upper level wind speeds for both simulations behave in the same fashion as the scatter plots of surface wind speeds. There is a large scatter between simulated and observed wind speeds and no clear bias in either direction. Generally, the simulations tend to predict vertical shape and change in speed as height increases. There is however,

no clear bias in either direction, again suggesting MM5 has an equally difficult time estimating upper air wind speeds as it did in estimating surface wind speeds. Wind directions for both simulations show good agreement with the discrepancies being less than 90°. NARR simulations appear to have more disagreement on October 24 and 25, but on a whole the simulations are able to predict the observed wind directions. Wind speed and direction have implications for the BlueSky framework as they control how fast (or slow) the smoke plumes and aerosols move in and out of specific areas and where they go. The agreement between the observed and the simulated surface and upper level wind directions allows the emissions from fires and smoke plumes be transported along the observed trajectories. Large scattering in the wind speeds will either speed up or delay the transport of smoke, resulting in errors in the timing of peak $PM_{2.5}$ concentrations at specific locations downwind.

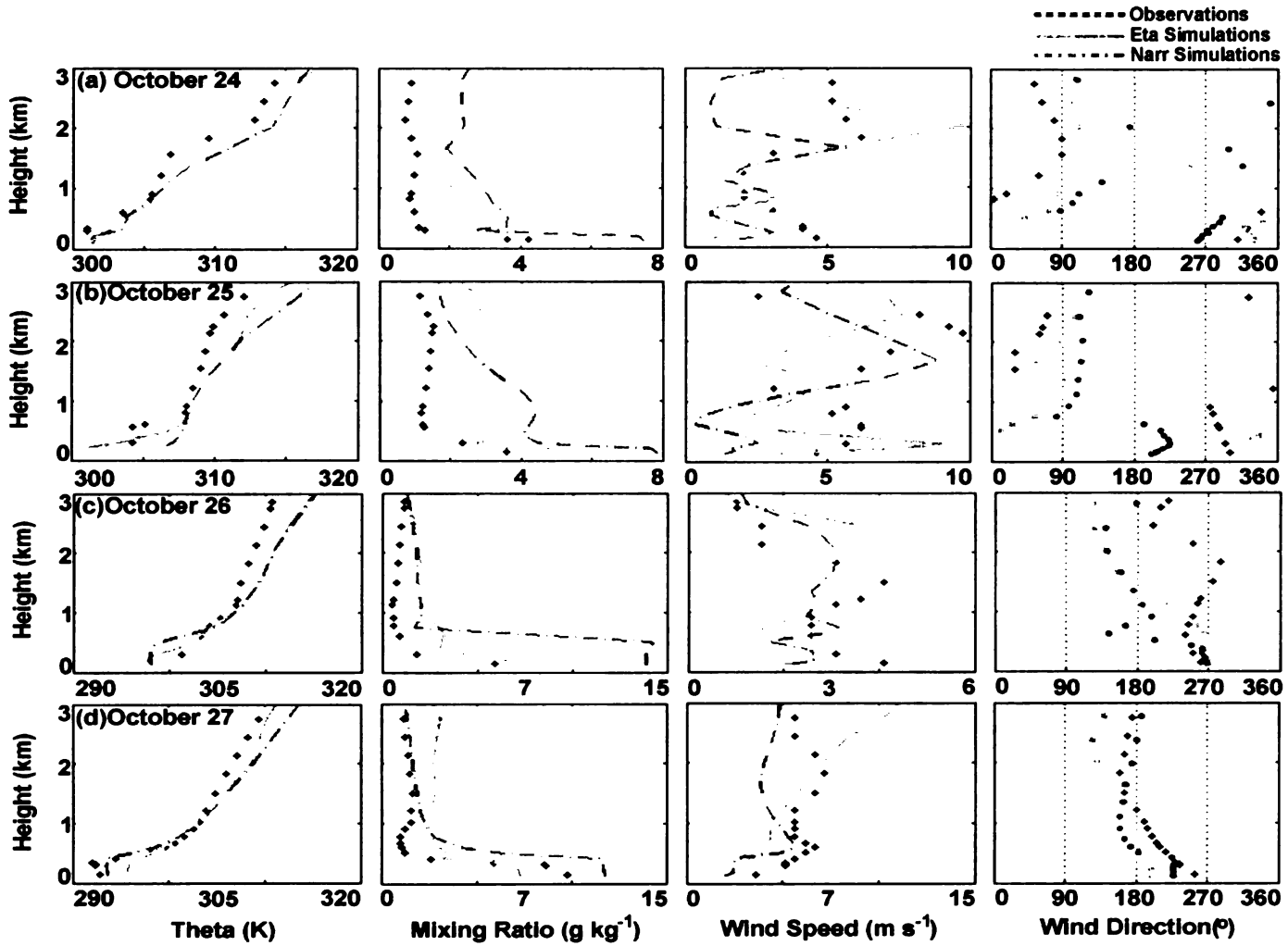

Figure 4.6 Comparison of upper level profiles at 1600 PST (00Z) at the San Diego, CA rawinsonde site. Black circles represent observations. Light gray solid lines and circles (wind direction) represent MM5 simulated meteorological conditions initialized with Eta output. Darker gray dashed lines and circles (wind direction) represent MM5 simulations initialized with NARR output.

Smoke Plume and $PM_{2.5}$ Predictions

Comparison of BlueSky predicted smoke plume orientation and shape with observations is shown in Figure 4.7 for October 24-27 for both the Eta and NARR simulations. In this figure, MODIS HMS images are compared with the BlueSky $PM_{2.5}$ hourly totals for 1300 PST to 2300 PST. This 11 hour period is the period of MODIS HMS detection where significant smoke plumes are recorded and analyzed (McNamara et al. 2004). Overall, BlueSky is able to predict both the shape and orientation of the observed smoke plumes. On October 24th and 25th, the Eta-BlueSky simulation appears to do a slightly better job of predicting the aerial extent of the smoke plume than the NARR-BlueSky simulation. Both simulations on this day predict the tongue of higher aerosol concentration along the coast of California, but compared to NARR-BlueSky, the Eta-BlueSky simulation better predicts the shape and magnitude of $PM_{2.5}$ concentration within the plume, indicated by the darker shading within the HMS image and warmer colors in the BlueSky image. The NARR upper level meteorological profile on this day (Figure 4.6a) indicates weaker estimations of wind speeds above 1.5km, most likely the cause of the inconsistencies between $PM_{2.5}$ concentrations and shape for the NARR-BlueSky simulation as weaker winds will delay smoke impacts. On October 25, both the Eta and NARR BlueSky simulations fail to predict the northern extent of the observed smoke plume, but the areas of highest $PM_{2.5}$ concentration again are consistent with those in MODIS HMS images. The NARR-BlueSky smoke estimations appear to be slightly more spatially condensed as the Eta-BlueSky run. Both runs predict an area in northern California of moderate (5-15 $\mu g\ m^{-3}$) $PM_{2.5}$ concentrations not seen in the HMS imagery.

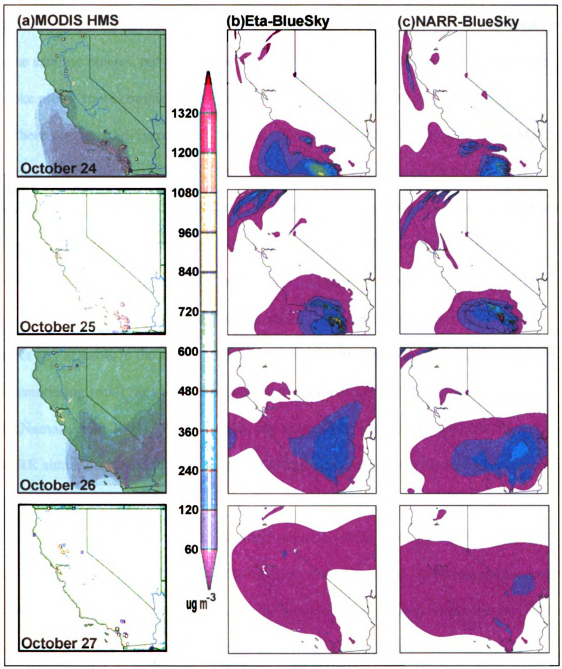

Figure 4.7 (a) Satellite images taken from the MODIS Hazard Mapping System (HMS) for October 24 – 27, 2007. Gray shading indicates significant smoke plumes. Darker shades of gray represent higher concentrations of smoke. Corresponding BlueSky images are total $PM_{2.5}$ concentrations for the same days for the hours of 1300 PST to 2300 PST for (b) Eta MM5 initialization data and (c) NARR MM5 initialization data. Warmer colors indicate higher concentrations of $PM_{2.5}$.

BlueSky images on October 26 again indicate the highest $PM_{2.5}$ peaks in similar locations to the satellite images, but the NARR-BlueSky run predicts the shape and extent of the smoke plume more completely, capturing the elevated concentrations of $PM_{2.5}$ in southern Nevada. Disagreements between observations and both Eta and NARR MM5 estimated wind directions above 1 km (Figure 4.6c) are apparent on October 26. However below 1 km, the NARR simulated wind directions agree with the observed wind directions, most likely causing this difference between the Eta and NARR-BlueSky smoke plume orientations. Both BlueSky runs simulate for October 27 $PM_{2.5}$ concentrations <5 $\mu g\ m^{-3}$ over most of the region. Although the HMS image does not detect any aerosols in the area on this day, MODIS is known to have difficulty differentiating small fires and subsequent smoke emissions from the background (McNamara et al. 2004). Winds on this day agree with observations for both Eta and NARR simulations, and most likely the moderate southerly winds (up to 3 km) helped remove the large aerosol concentrations from the region.

Figure 4.8 compares MODIS/GASP aerosol optical depth (AOD) images with BlueSky images at 1500 PST (2300 Z) on each of the four days. AOD images are used to establish a quantitative understanding of the aerosol concentrations within the air column to surface BlueSky predicted $PM_{2.5}$ concentrations. These images show that while BlueSky predicts similar increases of aerosols (specifically $PM_{2.5}$) as the AOD images, in reality there is much more variability in aerosol concentrations than BlueSky indicates. On October 24th, the NARR-BlueSky run simulates an increase in $PM_{2.5}$ off the coast of northern California, which is not seen in the Eta-BlueSky simulation. On October 25, the

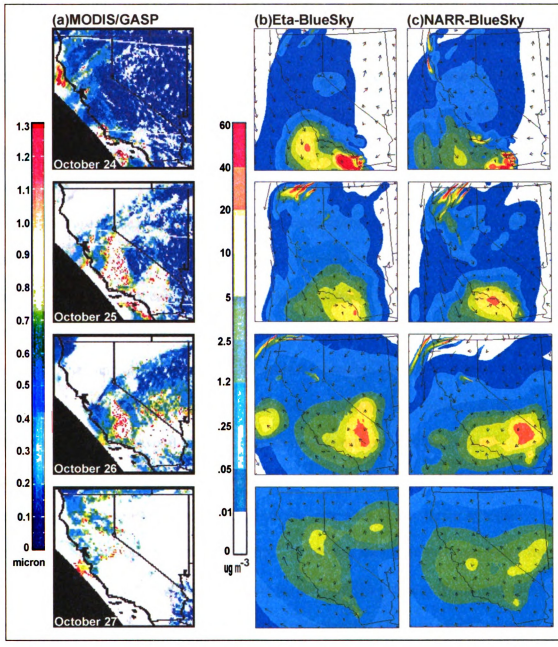

Figure 4.8 (a) MODIS/GASP Aerosol Optical Depth (AOD) images at 1500 PST (2300Z) for October 24 - 27, 2007 with corresponding BlueSky simulated smoke plumes for (b) Eta MM5 initialization data and (c) NARR MM5 initialization data. Warmer colors in the AOD images indicate areas of higher aerosol concentrations. Warmer colors within the BlueSky images indicate higher levels of surface $PM_{2.5}$ concentration.

Eta-BlueSky simulation is able to predict the larger increases in $PM_{2.5}$ off the coast of southern California. Both BlueSky simulations estimate large $PM_{2.5}$ increases over southern California on October 26, whereas the AOD images shows these increases further to the north, perhaps due to disagreements between simulated and observed wind speeds and directions (Figure 4.6c).

A quantitative evaluation of the BlueSky-predicted $PM_{2.5}$ concentrations is not as straightforward as the evaluation of predicted meteorological fields. $PM_{2.5}$ observations include not only the contribution of $PM_{2.5}$ due to wildland fires, but also a "background value" due to anthropogenic and natural sources. BlueSky $PM_{2.5}$ predictions however, only include the amount of $PM_{2.5}$ generated by wildland fires. Thus, a direct comparison of the modeled and observed concentrations is not possible because in theory, without the background value included, BlueSky predictions will always be smaller than the observations. While several methods may be used to estimate the background concentration, including running a photochemical model, Fusina *et al* (2007) calculated an average observed PM concentration from the same sites under similar synoptic conditions, but without the influence of fire. These averages were then subtracted from the observed PM concentrations during the period with fire activity. While this method is reasonable, it is difficult to find a time period experiencing identical synoptic conditions, and the results also can yield negative values which are difficult to interpret. In this study, instead of trying to calculate the background value, the time-rate changes of the simulated and observed surface $PM_{2.5}$ concentrations were compared. The rationale behind this approach is that a rapid rate of increase in concentration would indicate the influence of smoke plumes on a specific location.

Comparisons of time-rate change of BlueSky predicted surface $PM_{2.5}$ concentrations with observations for the Eta-BlueSky simulation are presented in Figure 4.9 and comparisons for the NARR-BlueSky simulation are in Figure 4.10 at four monitoring sites within the domain. Along with each station's time-rate change time series, Figures 4.9 and 4.10 show the surface meteorological comparisons and the station locations. A disadvantage of using single station time series in comparing $PM_{2.5}$ concentrations is the dependence of each station to the location of the simulated smoke plume. For instance, a simulated smoke plume may miss a station's location by only one model grid point and the expected increase in $PM_{2.5}$ is then not produced by the simulation, giving an impression that the BlueSky simulations to severely under-predict surface $PM_{2.5}$ concentrations. While this may be true, the under-prediction may also just be due to the "miss" of the smoke plume due to differences in the simulated and observed upper level meteorological patterns in wind speed and direction. For this reason, the comparison was made at the grid point closest to the observational site as well as at the four surrounding grid points (to the north, south, east and west).

Both Figure 4.9a and Figure 4.10a illustrate a natural variability of about ± 10 μg m^{-3} that exists within the observed $PM_{2.5}$ concentrations, since no smoke plumes passed this monitoring site during the seven days presented. This variability due to factors other than wildland fires makes it difficult to assess the ability of BlueSky to accurately predict the magnitude of smoke impacts, although BlueSky did correctly not simulate fire impacts during this period at the station located in Figures 4.9a and 4.10a. Using Figure 4.7 as a reference for smoke plume trajectories during October 24-27, Figures 4.9b and

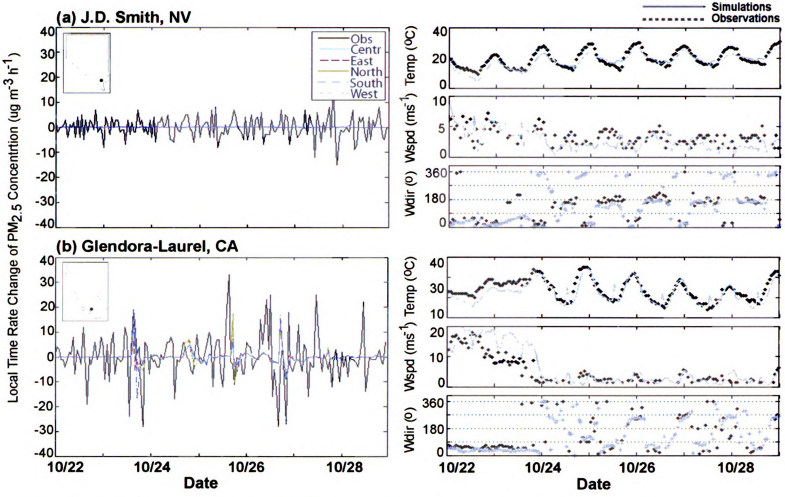

Figure 4.9 (Left) Eta simulated and observed local time rate change of $PM_{2.5}$ concentrations at four monitoring sites within the domain. Black lines represent observed $PM_{2.5}$ and colored lines represent BlueSky simulated $PM_{2.5}$ concentrations. (Right) Corresponding surface meteorological stations. Black triangles represent observations while gray lines and stars represent MM5 simulated temperature (Temp), wind speed (Wspd), and wind direction (Wdir).

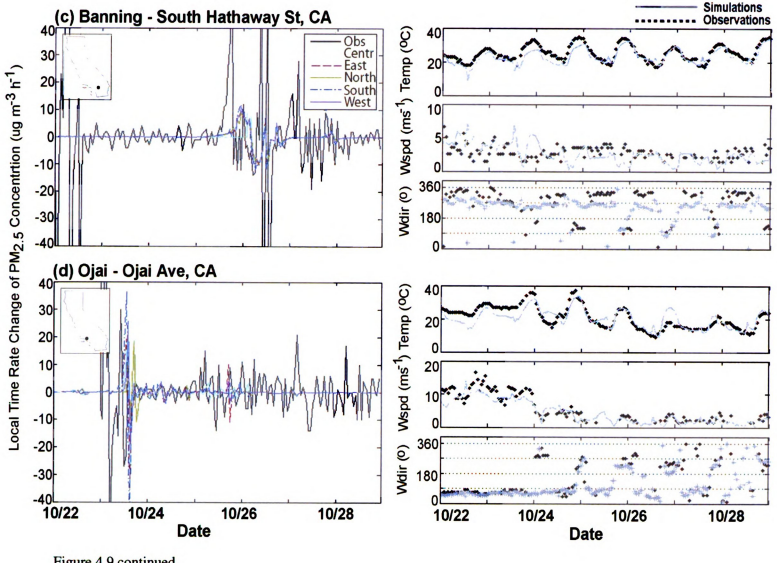

Figure 4.9 continued.

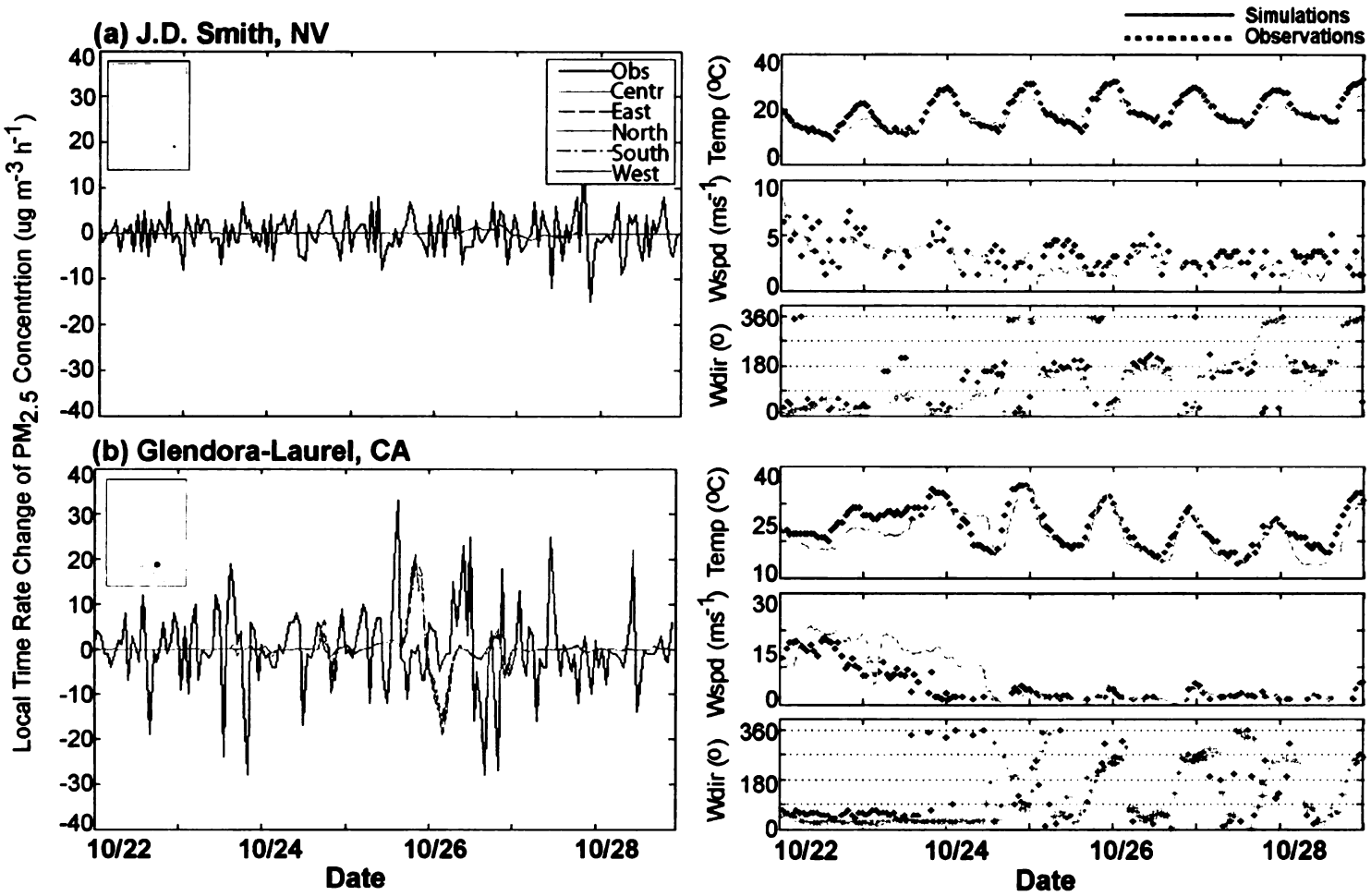

Figure 4.10 (Left) NARR simulated and observed local time rate change of $PM_{2.5}$ concentrations at four monitoring sites within the domain. Black lines represent observed $PM_{2.5}$ and colored lines represent BlueSky simulated $PM_{2.5}$ concentrations. (Right) Corresponding surface meteorological stations. Black triangles represent observations while gray lines and stars represent MM5 simulated temperature (Temp), wind speed (Wspd), and wind direction (Wdir).

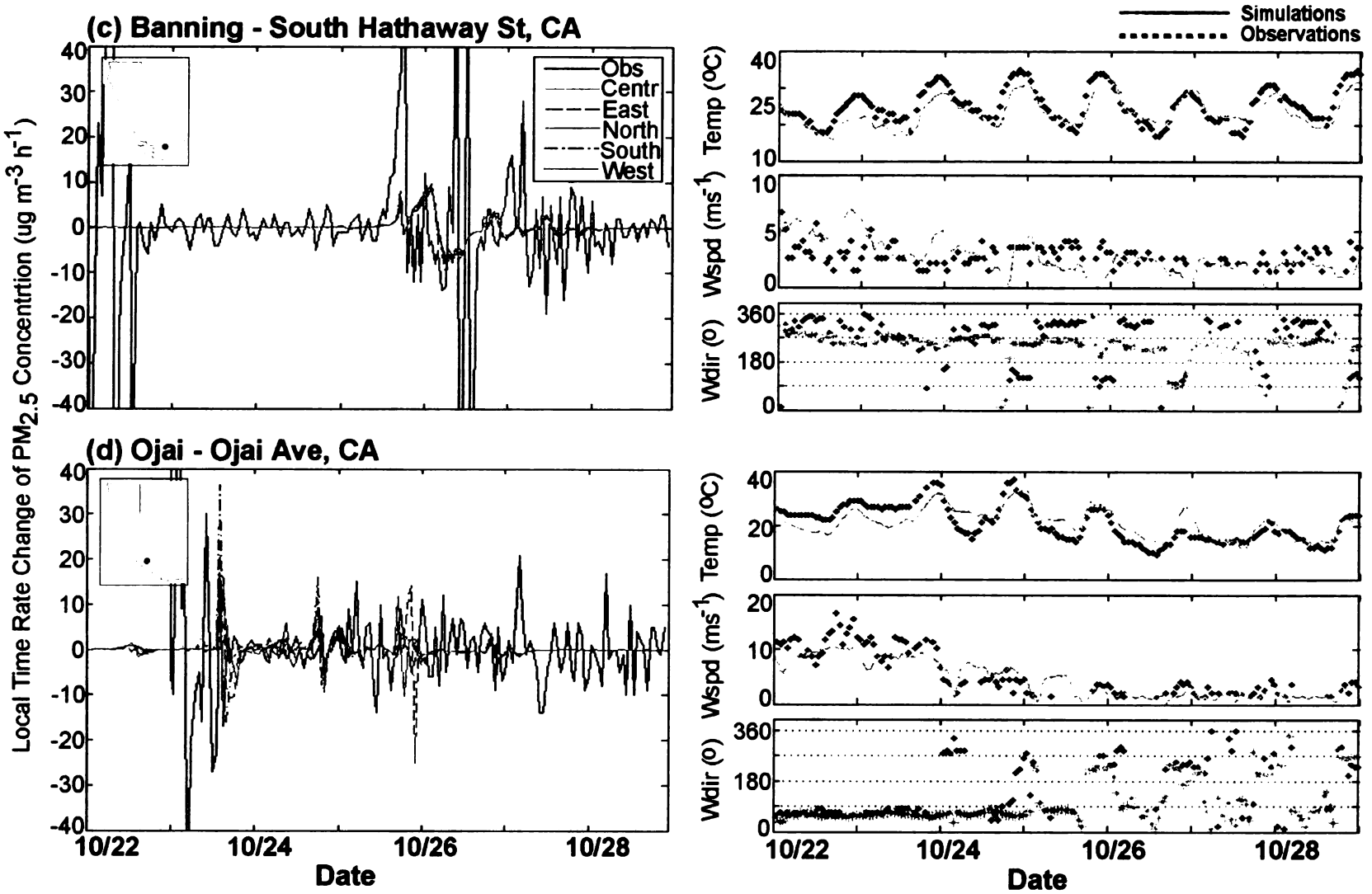

Figure 4.10 continued.

4.10b should show an increase in $PM_{2.5}$ on October 24th-26th and a slight increase on the 27th. At this station, both the Eta-BlueSky and NARR-BlueSky simulations capture the increases in $PM_{2.5}$ just before October 26th and again before October 27th, but the predicted magnitude is less than the observed on both days. On October 24th, however, while the Eta-BlueSky simulation is able to predict the timing and magnitude of the observed smoke impact, the NARR-BlueSky simulation does not. Simulated surface meteorology in both runs agree with observations, suggesting discrepancies may be due to disagreements in upper level wind speeds and directions (Figure 4.6). At the station in Figures 9c and 10c, smoke impacts were observed on October 26th and 27th as the smoke plume moved to the east. Both Eta and NARR BlueSky predictions again correctly simulate the timing and magnitude of the increase in $PM_{2.5}$ on the 26th, but fail to capture the larger increases found before and after this event. While both simulations do not predict the increase observed on October 25, the Eta-BlueSky run shows an increase in simulated $PM_{2.5}$ around midday on the 26th. The Eta-BlueSky run is able to predict the observed increase on October 27th however, the simulations predict this increase in $PM_{2.5}$ to be ~eight hours earlier. Discrepancies within MM5 upper level (3 km) wind speeds cause the simulated smoke plume to reach the station location earlier than the observations indicate. The station shown in Figures 9d and 10d indicates BlueSky correctly simulates an increase in $PM_{2.5}$, in magnitude and timing, near October 24th and 26th. On the 24th, the simulated smoke impact is delayed compared to observations, which is most likely a result of weaker simulated surface and upper level wind speeds.

Clearly, the timing and magnitude of BlueSky predictions were comparable to

observations when BlueSky did predict a smoke impact. However, BlueSky was not able to predict all of the large increases the observations indicated. Possible explanations include the randomness within the observations of $PM_{2.5}$ concentration such as the natural variability seen in Figures 9a and 10a. Other random factors are sudden, unrealistic increases in $PM_{2.5}$ concentrations. These sudden increases could be due a number of different things, an example being, a large bus passing by a monitor. The exhaust from the bus releases large amounts of pollutants into the air, increasing the aerosol concentration at that site at a particular time. While this does increase the amount of $PM_{2.5}$ at that particular time, it is not a true indication of the $PM_{2.5}$ levels during that day/hour. Other errors within the BlueSky simulations may be due to uncertainties within the emissions and dispersion models incorporated into the framework. Larkin *et al* (2007) explain that there is a high level of uncertainty with the fuel loadings used because they are usually unknown in the majority of wildfires. Consumption calculations also contain uncertainty as they are dependent upon fuel loadings.

Summary and conclusions

In early 2000, the USDA Forest Service AirFire team launched the BlueSky Smoke Modeling Framework to better predict wildland fire smoke plume dispersion and subsequent impacts. This system integrates meteorology, emissions, dispersion and trajectory models, and the simulations are made available to fire managers and air resource regulators. Originally designed as a tool for making 'go' and 'no-go' decisions for prescribed burns, BlueSky's applications have been expanded to include smoke impact assessments concerning wildland fire use (WFU) fires and wildfires. The purpose

of this study was two-fold: 1) evaluate BlueSky's ability to simulate smoke dispersion and surface $PM_{2.5}$ impacts from the October 2007 wildfires and 2) to assess BlueSky's sensitivity to different meteorological (MM5) initialization data sets.

The performance of the meteorological model (MM5) in simulating both surface and upper air variables was first evaluated. The simulations for both data sets predicted the trend and day-to-day variation that occurred due to changes in synoptic conditions. NARR surface temperatures were slightly warmer than Eta and both simulations created a warm bias at night and a cool bias during the day. These warm and cool biases create a smaller overall diurnal temperature range than what was actually observed. Mixing ratio between the two data sets are comparable, both exhibiting a moist bias throughout the day. Both Eta and NARR data sets tended to under predict surface wind speeds, but were able to predict accurate surface wind directions. At the upper levels, the simulations using the Eta initialization fields simulated better predictions of potential temperature, mixing ratio and wind speeds than the NARR initialization fields. Both data sets, however, show a warm, moist bias throughout the atmosphere. Important for transport simulations, both model runs were able to produce the observed change in wind directions with height.

After the meteorological comparisons were completed, comparisons of smoke plume shape and trajectory were analyzed. Results indicate the predicted smoke plumes using both MM5-Eta and MM5-NARR meteorological output to be in agreement with HMS satellite images, in both shape and orientation. For days that the simulated smoke plume did not match the satellite image, upper level observed and simulated wind directions were in disagreement. Comparisons between BlueSky and MODIS/GASP

Aerosol Optical Depth (AOD) images show BlueSky captures the peaks and locations of large aerosol concentrations but tends to estimate smaller aerial coverage and spatial variation when compared to the satellite observations.

Next, single station time series comparisons were analyzed. These time series comparisons were difficult to evaluate because smoke impacts in BlueSky are a result only of wildfires, while those in observations can be due to anthropogenic sources as well. To overcome this, the local time rate change of the hourly $PM_{2.5}$ concentration was used for comparison. A natural variability on the magnitude of about ± 10 $\mu g\ m^{-3}$ is apparent in the observed $PM_{2.5}$ concentrations. Timing and magnitude of BlueSky predicted surface $PM_{2.5}$ concentrations were comparable to observations when BlueSky did predict an increase in $PM_{2.5}$. However BlueSky was not able to predict all of the large increases in $PM_{2.5}$ the observations indicated. The prediction with MM5-Eta meteorology seemed to perform slightly better than NARR simulations, which may be due to slightly more surface and upper air disagreements within wind speed and wind direction in the MM5-NARR model run.

While BlueSky is useful for predicting smoke plume shape and transport, much more work needs to be done at improving the surface $PM_{2.5}$ concentration predictions. It is also clear that BlueSky is also dependent upon the accuracy of the meteorological forecasts, but because both runs still created differences between observed and simulated smoke impacts; neither initialization data set can be considered better than the other. Eta initialization data however, is available for real-time forecasting this data set could be more beneficial to fire managers.

PART V

CONCLUSIONS

Summary

Since the 1980's, the annual number of wildfires has decreased substantially (NIFC 2008). While the number of wildfires has steadily decreased, the average size of fires has increased, and the total numbers of acreage burned in the 2007 fire season, 9.3 million acres, was the second highest on record, behind only the 2006 totals (NCDC 2008). Wildfires are a beneficial component within the environment. Not only are they a necessary component of the carbon cycle, wildfires also promote regeneration and stimulation of the growth of many plant species, and aid in management of forest undergrowth. However, the smoke released from these fires can have adverse effects on surrounding communities. Decreased regional and local visibility, and potential impaired health conditions due to the air we breathe is cause for concern. To balance the positive and negative effects of wildfires, the Environmental Protection Agency (EPA) created air quality regulations and established limits for acceptable levels of any particular pollutant (EPA 2003).

In early 2000, the BlueSky Smoke Modeling Framework was developed (Berg et al. 2003). This framework links together meteorological, emissions, dispersion and trajectory models to provide fire managers with estimated locations and timing of wildland fire smoke impacts (Berg et al. 2003). Initially, BlueSky was designed with prescribed burning in mind and aimed assisting fire managers to make 'go' and 'no-go' decisions quickly and confidently. Recently, however, BlueSky has been modified and its use extended to the suppression and management of wildfires. This research project

was undertaken to validate BlueSky's ability to predict the timing and impacts of wildfire smoke. Observed $PM_{2.5}$ concentrations were collected from two separate case studies, northern California in August of 2006 and southern California in October of 2007, to compare with BlueSky estimated $PM_{2.5}$ concentrations. Both case studies represent large wildfire outbreaks, providing strong surface and satellite smoke footprints. Not only was this research focused on evaluating the accuracy of BlueSky predicted trajectory, timing and strength of smoke impacts but, it also assessed the sensitivity of BlueSky predictions on accurate meteorological inputs. Two sets of MM5 initialization data were used: NCEP 40 km Eta data and 32 km North American Regional Reanalysis (NARR) data.

Major findings of this research:

- MM5 is able to accurately simulate the observed temporal variations in surface temperatures, wind speeds and wind directions due to changes in synoptic conditions.
- MM5 is able to correctly estimate wind directions both at the surface as well as the observed changes as height increased.
- MM5 is able to simulate the upper level (up to 3 km) vertical profiles of wind speeds, but is not able to simulate the observed magnitudes of upper level or near-surface wind speeds.
- BlueSky is able to accurately predict regional patterns of wildfire smoke in both smoke plume orientation and aerial extent.
- Peak aerosol maximums within MODIS aerosol optical depth imagery align with peak BlueSky predicted $PM_{2.5}$ concentrations.

- Magnitudes of BlueSky predicted increases in surface $PM_{2.5}$ concentrations agree with the observed increases in $PM_{2.5}$, especially when the observed concentrations are greater than 10 $\mu g\ m^{-3}$. However, BlueSky is unable to predict all of the observed increases in surface $PM_{2.5}$ concentrations.
- BlueSky smoke prediction is proven to be sensitive to the meteorological inputs, but only small differences are produced in the BlueSky predictions driven by meteorological output produced with two different popular large-scale fields (Eta and NARR).

Overall, BlueSky proved to be a good tool for predicting long-range location of wildfire smoke plumes and their subsequent increases of surface $PM_{2.5}$ concentration, but had difficulty in predicting the overall magnitude of $PM_{2.5}$ increases. BlueSky was found to be sensitive to the input meteorology used, with slight differences in upper level wind patterns creating larger differences in the predicted and observed smoke impacts. While improvements to the emissions model and fire characteristic inputs are necessary for accurate predictions of the magnitudes of smoke impacts, BlueSky is still a useful tool for obtaining the overall location, size and path of a smoke plume and indicating the areas of possible large impacts. With this information, warnings can be issued to those regions within the smoke plume's path and cautionary steps can be taken to ensure the safety of the community.

Study Limitations

This study, like any research project, contains limitations that are summarized here. First, fire and climate effects are difficult to model because of the fine spatial scale necessary for useful, detailed results. Downscaling and/or upscaling model predictions and input data create assumptions that may not be accurate at the new scale. These assumptions are then propagated throughout the model and leads to uncertainties within the model results. These uncertainties affect the BlueSky system because as a whole, accurate smoke trajectory and concentration predictions are dependent upon the accuracy and reliability of all necessary inputs to each of the modeling system components. Error propagation due to model scaling is a limitation because, without confidence in model results, the evaluation efforts and usefulness of the study diminishes. Another limitation concerning fire and climate modeling is the need to balance simplicity in data input requirements for users with the detailed data input requirements needed for the complex framework components found within the BlueSky system. Complex computer models that are not user friendly are not likely to be employed by fire or land managers and air quality engineers, or if the models are indeed used, the input data may be incorrectly entered into the system, creating erroneous results. This balance between input simplicity and computer complexity is limiting because creating simpler models with less strict data input requirements may not be suitable for providing the needed output information for use in planned burn activities, air quality management or fire suppression strategies.

There were also limitations when trying to compare modeled and observed smoke trajectories and ground concentrations. One of the main limitations was the lack of an extensive $PM_{2.5}$ monitoring network in northern California. The available monitoring

network in northern California was restricted by the varying terrain that characterizes the region, and in turn created a sparse observing network. The sparse monitoring network in northern California made it difficult to accurately compare surface simulated $PM_{2.5}$ concentrations with observed concentrations. For instance, a simulated smoke plume may miss a station's location by only one model grid point and the expected increase in $PM_{2.5}$ is then not produced by the simulation, giving an impression that the BlueSky simulations to severely under-predict surface $PM_{2.5}$ concentrations. While this may be true, the under-prediction may also just be due to the "miss" of the smoke plume due to differences in the simulated and observed upper level meteorological patterns in wind speed and direction. A denser network would allow for a more comprehensive surface concentration analysis.

Comparison between satellite smoke plumes trajectory and concentration with BlueSky output was also limited by the available data. The MODIS Hazard Mapping System (HMS) archives only the 24 hour composites of the smoke evident each day within the full air column. BlueSky however, outputs are surface hourly images, thus, a direct comparison between the two is difficult. Composite images of BlueSky output can be created, however this increases the computer time needed to provide the smoke plume estimations to the users. In addition, the HMS satellite images do not give a quantitative measure of the aerosol concentrations within the plume, so a second database, in this case MODIS aerosol optical depth (AOD) images, needed to be employed.

Another source of limitations is the observed $PM_{2.5}$ concentrations contain not only $PM_{2.5}$ produced by fire emissions, but also contain $PM_{2.5}$ contributions from other natural and anthropogenic sources. BlueSky predicted concentrations of particulate

matter only consider the contributions from fire and not those due to natural or anthropogenic sources such as cars and industry. Because of this, direct comparison between BlueSky derived concentrations and observed concentrations was difficult as BlueSky concentrations will, theoretically, always be less than the observed.

Finally, there are limitations within the individual BlueSky model parameters themselves. For example, there is uncertainty associated with initialization data sets and the physical parameterizations used within the meteorological mesoscale model. These uncertainties are due to smoothing and estimating that occurs when trying to simulate real-world phenomena using physical equations. Also, there is uncertainty within the emissions and dispersion models used within the framework. Wildfires burn through multiple fuel loadings (ie. grasses, chaparral, trees, etc) and often times these fuel loadings are unknown. To obtain the fuel loadings for wildfires, BlueSky uses fuel classification reference databases (ie. FCCS, NFDRS). While these databases are based on reality, smoothing and estimation is used to create complete spatial coverage. Error and uncertainty within fuel loadings propagate into the consumption calculations, as these calculations are dependent upon fuel loadings.

Future Work

Although the BlueSky smoke modeling framework is operational in many parts of the country, more work needs to be done in order to improve the accuracy of its predictions. One major improvement would be the creation and implementation of a nationally-consistent wildland fire (including both wildfires and prescribed fires) reporting system. This reporting system would allow for increased reliability and

timeliness of wildland fire input data for all regions within the United States. Currently, because no consistent reporting system exists, BlueSky inputs are different depending on the region, making it difficult to validate the models accuracy.

Equally important is an expansive and geographically representative $PM_{2.5}$ monitoring network. This network would need to cover the entire United States, with an emphasis on rural areas were prescribed burning typically occurs, and mountainous regions where wildfires often start. Currently, $PM_{2.5}$ monitoring networks are regionally diverse, such that some areas have expansive networks (southern California) while other areas have sparse networks (northern California). These monitoring networks will not only help to better monitor aerosol and pollutant levels in the atmosphere, but they will allow for easier and better comparison with surface BlueSky $PM_{2.5}$ estimations, and ultimately help to improve the accuracy and reliability of these estimations.

The BlueSky smoke modeling system as a whole needs further validation and evaluation of its individual components. This study found that mesoscale meteorology forecasting using the PSU/NCAR Mesoscale Model (MM5) provided accurate three-dimensional meteorological fields as well as their temporal variations for use in BlueSky dispersion modeling. However, a study by BSRW (2006), found that the model was causing unrealistic collapses of the mixing height. These findings imply that further improvement to the mesoscale models boundary layer scheme is necessary. Experimenting with different model parameterizations, whether in the meteorological model or the emissions model, makes clear the importance and sensitivity the accuracy of that particular model has on the overall smoke concentration estimations. Jain *et al* (2007) also suggests ensemble techniques should be employed to see whether the models

themselves increase the relative success or failure of the BlueSky framework (Jain et al. 2007). To date, no BlueSky studies on the remaining framework components have been evaluated (fire emissions, dispersion and trajectory models) to compare their estimations with reality. Also, an evaluation switching BlueSky's emission model from EPM, a model originally designed with prescribed burn in mind, to one that includes smoldering and the consumption of live fuels, such as the fire production emission simulator (FEPS) has also been suggested (Berg et al. 2003). Errors that occur in any of BlueSky's components are propagated throughout the rest of the framework and appear in the smoke estimations. Only accurate results in each component can produce reliable and accurate results from the framework as a whole.

REFERENCES

Achtemeier, G. L. 2005. Planned Burn-Piedmont. A local operational numerical meteorological model for tracking smoke on the ground at night: model development and sensitivity tests. *International Journal of Wildland Fire* 14 (1):85-98.

Adkins, J. W., S. M. O'Neill, M. Rorig, S. A. Ferguson, C. M. Berg, and J. L. Hoadley. 2003. Assessing the Accuracy of the BlueSky Smoke Modeling Framework During Wildfire Events. Paper read at 5th Symposium on Fire and Forest Meteorology and the 2nd International Wildland Fire Ecology and Fire Management Congress, at Orlando, FL.

Agency, U. S. E. P. 2006. 2006-2011 Strategic Plan: Charting Our Course, 184: U.S Environmental Protection Agency.

Andrews, P. L., and L. P. Queen. 2001. Fire modeling and information system technology. *International Journal of Wildland Fire* 10 (3-4):343-352.

Archibold, R. C. 2007. California Fires Destroy Scores of Homes. *The New York Times*, Oct 22, 2007.

Association, A. L. 2007. American Lung Association State of the Air Report: 2007: American Lung Association.

Bacon, D. P., N. N. Ahmad, Z. Boybeyi, T. J. Dunn, M. S. Hall, P. C. S. Lee, R. A. Sarma, M. D. Turner, K. T. Waight, S. H. Young, and J. W. Zack. 2000. A dynamically adapting weather and dispersion model: The Operational Multiscale Environment Model with Grid Adaptivity (OMEGA). *Monthly Weather Review* 128 (7):2044-2076.

Berg, C. M., S. M. O'Neill, S. A. Ferguson, and J. W. Adkins. 2003. Application of the BlueSky Smoke Modeling Framework to the Rex Creek Wildfire. Paper read at 5th Symposium on Fire and Forest Meteorology and the 2nd International Wildland Fire Ecology and Fire Management Congress, at Orlando, FL.

Binkowski, F. S., and S. J. Roselle. 2003. Models-3 community multiscale air quality (CMAQ) model aerosol component - 1. Model description. *Journal of Geophysical Research-Atmospheres* 108 (D6):-.

Breyfogle, S., and S. A. Ferguson. 1996. User Assessment of Smoke-Dispersion Models for Wildland Biomass Burning, 30: US Department of Agriculture: General Technical Report PNW-GTR-379.

BSRW. 2006. BlueSkyRAINS West (BSRW) Demonstration Project: Final Report 2006, 38: US Department of Agriculture.

Cohen, J. D., and J. E. Deeming. 1985. The National Fire-Danger Rating System: Basic Equations, 16: PSW GTR PSW 82.

Craig, K. J., N. J. M. Wheeler, S. B. Reid, E. K. Gilliland, and D. C. Sullivan. 2007. Development and Operation of National CMAG-based PM2.5 Forecast System for Fire Management. Paper read at 6th Annual CMAS Conference, October 1-3, at Chapel Hill, NC.

Draxler, R. R., and G. D. Hess. 1997. Description of the HYSPLIT-4 modeling system.

Durrenberger, R. W. 1959. *The geography of California in essays and readings*: Brewster Pub. Co.

———. 1968. *Elements of California geography*: National Press Books.

EPA. 2003. Air Quality Criteria for Particulate Matter: Fourth External Review: Environmental Protection Agency.

Evers, L. 2006. BlueSky Proves Its Value in Predicting Smoke. *USDA Fire Management Today* 66 (3):9-11.

Evers, L., S. Ferguson, S. O'Neill, and J. Hoadley. 2006. Applying BlueSky Smoke Modeling Framework on Wildland Fires. *USDA Fire Management Today* 66 (3):5-8.

Ferguson, S. A., J. Peterson, and A. Acheson. 2001. Automated, Real-Time Predictions of Cumulative Smoke Impacts From Prescribed Forest and Agricultural Fires. Paper read at 4th Symposium on Fire and Forest Meteorology, 13-15 November, at Reno, NV.

Flaccus, G. 2007. 1,500 homes lost; $1B loss in San Diego area. *The Associated Press; Seattle Times*, Oct 24, 2007.

Fusina, L., S. Zhong, J. Koracin, T. Brown, A. Esperanza, L. Tarney, and H. Preisler. 2007. Validation of BlueSky Smoke Prediction System Using Surface and Satellite Observations During Major Wildland Fire Events in Northern California. Paper read at The fire environment - innovations, management, and policy; conference proceedings, at Destin, FL.

Grell, G. A., J. Dudhia, and D. R. Stauffer. 1994. A Description of the Fifth-Generation Penn State/NCAR Mesoscale Model (MM5). NCAR Technical Note TN-398, June, 1994

Hardy, C., J. P. Menakis, D. G. Long, and J. L. Garner. 1998. FMI/WESTAR Emissions Inventory and Spatial Data for the Western United States. Missoula, Montana: USDA Forest Service, Rocky Mountain Research Station, Fire Sciences Laboratory.

Hummel, J., and J. Rafsnider. 1995. TSARS plus Smoke Production and Dispersion model User's Guide. Ft Collins, CO: Unpublished report on file with Environment Science and Technology Center.

Jain, R., J. Vaughan, H. Kyle, C. Ramosa, C. Clalborn, S. Maarten, M. Schaaf, and B. Lamb. 2007. Development of the ClearSky smoke dispersion forecast system for agricultural field burning in the Pacific Northwest. *Atmospheric Environment* 41 (32):6745-6761.

Kim, D., and W. R. Stockwell. 2007. An online coupled meteorological and air quality modeling study of the effect of complex terrain on the regional transport and transformation of air pollutants over the Western United States. *Atmospheric Environment* 41 (11):2319-2334.

Larkin, N. K., S. M. O'Neill, R. Soloman, C. Krull, S. Raffuse, M. Rorig, J. Peterson, and S. A. Ferguson. 2007. The BlueSky Smoke Modeling Framework. *(Submitted).*

Lavdas, L. 1996. Program VSMOKE -- User's Manual. Asheville, N.C.: USDA Forest Service General Technical Report SRS-6.

Liu, Y. Q., G. L. Achtemeier, and S. Goodrick. 2006. Modeling Air Quality Effects of Prescribed Burn in Georgia with CMAQ-Daysmoke. Paper read at Proceedings of the Workshop on Agricultural Air Quality, ESA.

Lopes, A. G., M. G. Cruz, and D. X. Viegas. 2002. FireStation - An Integrated Software System for the Numerical Simulation of Fire Spread on Complex Topography. *Environmental Modeling & Software* ***17***:269-285.

Malm, W. C., D. E. Day, and S. M. Kreidenweis. 2000. Light scattering characteristics of aerosols as a function of relative humidity: Part I - A comparison of measured scattering and aerosol concentrations using the theoretical models. *Journal of the Air & Waste Management Association* 50 (5):686-700.

McGrattan, K. B. 2003. Smoke plume trajectory modeling. *Spill Science & Technology Bulletin* 8 (4):367-372.

McKenzie, D., S. M. O'Neill, N. K. Larkin, and R. A. Norheim. 2006. Integrating models to predict regional haze from wildland fire. *Ecological Modelling* 199 (3):278-288.

McKenzie, D., C. L. Raymond, L. K. B. Kellogg, R. A. Norheim, A. G. Andreu, A. C. Bayard, K. E. Kopper, and E. Elman. 2007. Mapping fuels at multiple scales: landscape application of the Fuel Characteristic Classification System. *Canadian Journal of Forest Research-Revue Canadienne De Recherche Forestiere* 37 (12):2421-2437.

McNamara, D., G. Stephens, M. Ruminski, and T. Kasheta. 2004. The Hazard Mapping System (HMS) - NOAA's Multi-Sensor Fire and Smoke Detection Program Using Environmental Satellites. In *13th Conference on Satellite Meteorology and Oceanograhy*. Norfolk, VA.

Minnich, R. A. 1987. Fire Behavior In Southern California Chaparral Before Fire Control: The Mount Wilson Burns at the Turn of the Century. *Annals of the Association of American Geographers* 77 (4):599-618.

Miranda, A. I. 2004. An integrated numerical system to estimate air quality effects of forest fires. *International Journal of Wildland Fire* 13 (2):217-226.

Miranda, A. I., C. Borrego, and D. X. Viegas. 1994. Forest Fire Effects On The Air Quality. *Air Pollution II, computer simulation*:191-199.

NCDC. 2008. Climate of 2007: Wildfire Season Summary at http://www.ncdc.noaa.gov/oa/climate/research/2007/fire07.html

NIFC. 2008. Fire Information: Available at: http://www.nifc.gov/.

O'Neill, S. M., S. A. Ferguson, and J. Peterson. 2003. The BlueSky Smoke Modeling Framework (www.BlueSkyRAINS.org). Paper read at 5th Symposium on Fire and Forest Meteorology and the 2nd International Wildland Fire Ecology and Fire Management Congress, at Orlando, FL.

O'Neill, S. M., J. L. Hoadley, S. A. Ferguson, R. Soloman, J. Peterson, N. K. Larkin, R. Wilson, D. Matheny, and R. S. Peterson. 2005. Applications of the BlueSkyRAINS Smoke Prediction System. In *EM Magazine*, 20-23.

Odion, D. C., E. J. Frost, J. R. Strittholt, H. Jiang, D. A. Dellasala, and M. A. Moritz. 2004. Patterns of fire severity and forest conditions in the western Klamath Mountains, California. *Conservation Biology* 18 (4):927-936.

Potter, B. E., N. Larkin, and N. Nikolov. 2006. Smoke, Fire and Weather: What Forest Service Research is Doing To Help. *USDA Fire Management Today* 66 (3):12-16.

Pouliot, G., T. Pierce, W. Benjey, S. M. O'Neill, and S. A. Ferguson. 2005. WIldfire Emission Modeling: Integrating BlueSky and SMOKE. Paper read at 14th International Emission Inventory Conference, at Las Vegas, NV.

Rapp, V. 2006. A Clear Picture of Smoke: BlueSky Smoke Forecasting. In *Science Update 14*, 12. Portland, OR: U.S. Department of Agriculture, Forest Service, Pacific Northwest Research Station.

Reinhardt, E. D., R. E. Keane, and J. K. Brown. 2001. Modeling fire effects. *International Journal of Wildland Fire* 10 (3-4):373-380.

Reza, H. G., J. Leovy, and A. Pham. 2007. Scale of the fires' disruption on display at San Diego Stadium. In *Los Anglese Times*. San Diego.

Sandberg, D. V., and J. Peterson. 1984. A source-strength model for prescribed fires in coniferous logging slash. Paper read at Proceedings: 21st Annual Meeting of the Air Pollution Control Association, Pacific Northwest International Section, at Pittsburgh, PA: Air Pollution Control Association.

Scire, J. S., F. R. Robe, M. E. Fernau, and R. J. Yamartino. 2000. A User's Guide for the CALMET Meteorological Model (version 5). Concord, MA: Earth Tech Inc.

Scire, J. S., D. G. Strimaitis, and R. J. Yamartino. 2000. A User's Guide for the CALPUFF dispersion model, version 5. Earth Tech. Inc. Concord, MA.

Sestak, M., S. O'Neill, S. Ferguson, J. Ching, and D. G. Fox. 2002. Integration of Wildfire Emissions into Models - 3/CMAQ with the Prototypes: Commnity Smoke Emissions Modeling System (CSEM) and BlueSKy. Paper read at 1st CMAS Model-3 User's Conference, at Research Triangle Park, NC.

Sestak, M. L., and A. R. Riebau. 1988. SASEM Simple Approach Smoke Estimation Model: USDI Bureau of Land Management Technical Note 382.

Valente, J., A. I. Miranda, A. G. Lopes, C. Borrego, D. X. Viegas, and M. Lopes. 2007. Local-scale modelling system to simulate smoke dispersion. *International Journal of Wildland Fire* 16 (2):196-203.

WRAP, and WGA. 2005. 2002 Fire Emission Inventory for the WRAP Region - Phase II: Western Regional Air Partnership and Western Governors Association.

WRAP, W. R. A. P. a. W. G. A. 2005. 2002 Fire Emission Inventory for the WRAP Region - Phase II.

WRCC. 2008. Southern California Climate Summaries (Western Regional Climate Center) available at: http://www.wrcc.dri.edu.

Zhong, S. Y., H. J. In, and C. Clements. 2007. Impact of turbulence, land surface, and radiation parameterizations on simulated boundary layer properties in a coastal environment. *Journal of Geophysical Research-Atmospheres* 112 (D13):-.